

---

**Research Article: New Research | Cognition and Behavior**

## **Pain-related fear – Dissociable neural sources of different fear constructs**

**Michael Lukas Meier<sup>1</sup>, Andrea Vrana<sup>1</sup>, Barry Kim Humphreys<sup>1</sup>, Erich Seifritz<sup>2</sup>, Philipp Stämpfli<sup>2,3</sup> and Petra Schweinhardt<sup>1,4</sup>**

<sup>1</sup>*Integrative Spinal Research, Department of Chiropractic Medicine, University Hospital Balgrist, Zurich, Switzerland*

<sup>2</sup>*Department of Psychiatry, Psychotherapy and Psychosomatics, Hospital of Psychiatry, University of Zurich, Zurich, Switzerland*

<sup>3</sup>*MR-Center of the Psychiatric Hospital, University of Zurich, Zurich, Switzerland*

<sup>4</sup>*Alan Edwards Center for Research on Pain, McGill University, Montreal, Canada*

<https://doi.org/10.1523/ENEURO.0107-18.2018>

Received: 21 March 2018

Revised: 3 September 2018

Accepted: 30 **October** 2018

Published: 26 December 2018

---

**Author contributions:** MLM designed research, performed research, analyzed data, wrote the paper; AV designed research, performed research, wrote the paper; BKH designed research, wrote the paper; ES designed research, performed research; PSt designed research, performed research, wrote the paper; PSc performed research, analyzed data, wrote the paper.

The authors declare no competing financial interests.

Corresponding author: Michael L. Meier, Balgrist, Campus, Lengghalde 5, 8008 Zurich, Switzerland. Phone: +41 44 510 73 80; E-mail: [michael.meier@balgrist.ch](mailto:michael.meier@balgrist.ch).

**Cite as:** eNeuro 2018; 10.1523/ENEURO.0107-18.2018

**Alerts:** Sign up at [www.eneuro.org/alerts](http://www.eneuro.org/alerts) to receive customized email alerts when the fully formatted version of this article is published.

Accepted manuscripts are peer-reviewed but have not been through the copyediting, formatting, or proofreading process.

Copyright © 2018 Meier et al.

This is an open-access article distributed under the terms of the Creative Commons Attribution 4.0 International license, which permits unrestricted use, distribution and reproduction in any medium provided that the original work is properly attributed.

1 **Pain-related fear – Dissociable neural sources of different fear constructs**

2

3 Abbreviated title: Neural dissection of pain-related fear constructs

4

5 Michael Lukas Meier<sup>1\*</sup>, Andrea Vrana<sup>1</sup>, Barry Kim Humphreys<sup>1</sup>, Erich Seifritz<sup>2</sup>,  
6 Philipp Stämpfli<sup>2,3</sup>, Petra Schweinhardt<sup>1,4</sup>

7 1) Integrative Spinal Research, Department of Chiropractic Medicine, University Hospital  
8 Balgrist, Zurich, Switzerland

9 2) Department of Psychiatry, Psychotherapy and Psychosomatics, Hospital of Psychiatry,  
10 University of Zurich, Zurich, Switzerland

11 3) MR-Center of the Psychiatric Hospital, University of Zurich, Zurich, Switzerland

12 4) Alan Edwards Center for Research on Pain, McGill University, Montreal, Canada

13 \* Corresponding author: Michael L. Meier, Balgrist, Campus, Lengghalde 5, 8008 Zurich,  
14 Switzerland

15 Mail: michael.meier@balgrist.ch

16 Phone: +41 44 510 73 80

17 Keywords (meSH): Amygdala, Machine Learning, Multivariate Analysis, Chronic Pain, Low  
18 Back Pain, Fear Network

19 Number of pages: 45

20 Number of figures: 1

21 Number of tables: 4

22 Number of words: Abstract (237), Significant statement (108), Introduction (628), Discussion  
23 (2355)

24

25

26 **Author contributions**

27 MLM designed research, performed research, analyzed data, wrote the paper

28 AV designed research, performed research, wrote the paper

29 BKH designed research, wrote the paper

30 ES designed research, performed research

31 PSt designed research, performed research, wrote the paper

32 PSc performed research, analyzed data, wrote the paper

33 **Acknowledgements**

34 We would like to thank Dr. Nina Kreddig (Ruhr University Bochum, Germany) and Dr. Stefan  
35 Sommer (ETH Zurich, Switzerland) for their intellectual contributions. Finally, we thank Sergio  
36 Maffioletti from S3IT (University of Zurich, Switzerland) for technical support regarding the  
37 supercomputing environment.

38 **Conflicts of interest**

39 The authors declare no competing financial interests.

40 **Funding sources**

41 This work was supported by the Foundation for the Education of Chiropractors and the Balgrist  
42 Foundation, Switzerland.

43

44

45

46

47

48

49 **Abstract**

50 Fear of pain demonstrates significant prognostic value regarding the development of persistent  
51 musculoskeletal pain and disability. Its assessment often relies on self-report measures of pain-  
52 related fear by a variety of questionnaires. However, based either on “fear of  
53 movement/(re)injury/kinesiophobia”, “fear avoidance beliefs” or “pain anxiety”, pain-related  
54 fear constructs plausibly differ while it is unclear how specific the questionnaires are in assessing  
55 these different constructs. Furthermore, the relationship of pain-related fear to other anxiety  
56 measures such as state or trait anxiety remains ambiguous. Advances in neuroimaging such as  
57 machine learning on brain activity patterns recorded by functional magnetic resonance imaging  
58 might help to dissect commonalities or differences across pain-related fear constructs. We  
59 applied a pattern regression approach in 20 human patients with non-specific chronic low back  
60 pain to reveal predictive relationships between fear-related neural pattern information and  
61 different pain-related fear questionnaires. More specifically, the applied Multiple Kernel  
62 Learning approach allowed generating models to predict the questionnaire scores based on a  
63 hierarchical ranking of fear-related neural patterns induced by viewing videos of activities  
64 potentially harmful for the back. We sought to find evidence for or against overlapping pain-  
65 related fear constructs by comparing the questionnaire prediction models according to their  
66 predictive abilities and associated neural contributors. By demonstrating evidence of non-  
67 overlapping neural predictors within fear processing regions, the results underpin the diversity of  
68 pain-related fear constructs. This neuroscientific approach might ultimately help to further  
69 understand and dissect psychological pain-related fear constructs.

70

71

72 **Significance**

73 Pain-related fear, often assessed through self-reports such as questionnaires, has shown  
74 prognostic value and clinical utility for a variety of musculoskeletal pain disorders. However, it  
75 remains difficult to determine a common underlying construct of pain-related fear due to several  
76 proposed constructs among questionnaires. The current study describes a novel neuroscientific  
77 approach using machine learning of neural patterns within the fear circuit of chronic low back  
78 pain patients that has the potential to identify neural commonalities or differences among the  
79 various constructs. Ultimately, this approach might afford a deeper understanding of the  
80 suggested constructs and might be also applied to other domains where ambiguity exists between  
81 different psychological constructs.

82

83

84

85

86

87

88

89

90

91       **1. Introduction**

92       Self-report measures of emotional states are paramount for behavioral neuroscience by enabling  
93       the understanding of brain response patterns (Shrout et al., 2017). However, the validity of self-  
94       reports is limited (Choi and Pak, 2005), probably also because often overlapping psychological  
95       constructs are assessed, illustrated by the fact that various questionnaires attempt to assess  
96       related constructs. One example is pain-related fear (PRF), which is a major explanatory variable  
97       of disability in patients with persistent musculoskeletal pain (Crombez et al., 1999; Vlaeyen and  
98       Linton, 2000; Vlaeyen et al., 2016). For the assessment of PRF, various questionnaires exist  
99       based on potentially different constructs such as fear of movement/(re)injury/kinesiophobia, fear  
100       avoidance beliefs or pain anxiety. There is an open debate on what their scores reflect on the  
101       fear-anxiety spectrum (Lundberg et al., 2011; Caneiro et al., 2017). Fear represents a reaction to  
102       an imminent threat, preparing the individual for “fight-flight-freeze”, whereas anxiety is  
103       described as more diffuse (e.g. cognitions about a future threat) (Kreddig and Hasenbring, 2017;  
104       LeDoux and Pine, 2016). While PRF questionnaires do not clearly distinguish between these  
105       emotions (Kreddig and Hasenbring, 2017; Lundberg et al., 2011), brain research provides  
106       evidence for a functional differentiation of fear and anxiety. Both emotions are controlled by the  
107       fear circuit (Tovote et al., 2015), however, subcortical regions (e.g. the amygdala) seem to be  
108       more involved in fast and defensive fear reactions (short defensive distance to threat) while  
109       cortical regions (e.g. the prefrontal cortex) are more likely responsible for complex cognitions of  
110       anxiety (large defensive distance to threat) (Qi et al., 2018; McNaughton and Corr, 2004).  
111       Therefore, advances in neuroimaging enable exploring the (sub-)cortical contributions to PRF  
112       constructs by examining interrelations between self-reported emotional states and brain response  
113       patterns. Specifically, machine learning techniques such as multivariate pattern analysis (MVPA)

114 applied to functional magnetic resonance imaging (fMRI) data make it possible to directly study  
115 the predictive relationship between a content-selective cognitive or emotional state (expressed as  
116 a label) and corresponding multivoxel fMRI activity patterns (Haynes, 2015; Hebart and Baker,  
117 2017). The label may have discrete (classification) or continuous (regression) values such as  
118 questionnaire scores (Formisano et al., 2008). Back straining activities (i.e. bending and lifting)  
119 are the most feared and pain-provoking movements among people with low back pain (LBP),  
120 based on ratings of perceived harmfulness or physiological responses (Caneiro et al., 2017;  
121 Leeuw et al., 2007a; Stevens et al., 2016; Glombiewski et al., 2015). As such, bending and  
122 lifting, either active or passive (e.g. through pictures) have been frequently used to provoke PRF  
123 (Leeuw et al., 2007c; Caneiro et al., 2017; Barke et al., 2016; Trost et al., 2009). Therefore, we  
124 provoked PRF by presenting video clips of daily activities including bending and lifting (harmful  
125 condition) and harmless activities such as walking (harmless condition) in a sample of 20 non-  
126 specific chronic LBP patients. We applied a pattern regression analysis in combination with  
127 Multiple Kernel Learning to assess potential neural predictors of the various PRF constructs  
128 based on weighting of 1) harmful and harmless conditions (condition weights) and 2) pattern  
129 information within sub-cortical and cortical fear processing regions (region weights). We first  
130 contrasted the different PRF questionnaires in terms of their model performance, namely the  
131 model's ability to predict the questionnaires scores based on brain response patterns across fear  
132 processing regions. Second, we compared the different prediction models according to the  
133 distributions of their condition and region weights to explore potential neural commonalities or  
134 differences of related PRF constructs. If the PRF questionnaires share overlapping PRF  
135 constructs, then the regions weights should be similarly distributed across fear processing  
136 regions. Conversely, if the contributing brain regions vary across the prediction models, this

137 would provide evidence for non-overlapping PRF constructs across questionnaires. Ultimately,  
138 this approach might help to further understand and dissect the various PRF constructs in chronic  
139 LBP.

## 140 **2. Methods**

### 141 **2.1 Patients**

142 The study was approved by the Ethics Committee Zurich (Switzerland) and all patients provided  
143 written informed consent before participation. The study was conducted in accordance with the  
144 Declaration of Helsinki. We recruited a total of 20 patients (mean age = 39.35 years, SD = 13.97  
145 years, 7 females, Table 1) with non-specific chronic LBP, considered a complex biopsychosocial  
146 condition (Maher et al., 2017; Deyo and Weinstein, 2001). Patients were recruited via local  
147 chiropractic and physiotherapy centres as well as via online advertisements. Inclusion criteria  
148 were low back pain of at least 6 months duration and age between 18 and 65 years. Exclusion  
149 criteria were a history of psychiatric or neurological disorders and specific causes for the pain  
150 (e.g. infection, tumour, fracture, inflammatory disease) that were ruled out by an experienced  
151 clinician.

### 152 **2.2 Self-report measures of pain-related fear**

153 PRF was assessed using several questionnaires:

154 (1) The Tampa Scale of Kinesiophobia questionnaire (TSK) (Vlaeyen et al., 1995; Kori et al.,  
155 1990) was used to assess fear of movement/(re)injury and kinesiophobia. The 17-item German  
156 version of the TSK (TSK-17) with satisfactory internal consistency (Cronbach's  $\alpha = 0.76-0.84$ )  
157 contains statements focusing on fear of physical activity rated on a 4-point Likert scale from 1 =

158 “strongly disagree” to 4 = “strongly agree” (Rusu et al., 2014). Due to additional versions of  
159 original 17-item TSK questionnaire, we also calculated the questionnaire scores of the 13- and  
160 11-item TSK versions (TSK-13, TSK-11). The 13-and 11-item versions were previously  
161 validated by confirmatory factor analysis and demonstrated acceptable levels of internal  
162 consistency (Cronbach’s  $\alpha = 0.80$ ) (Goubert et al., 2004; Tkachuk and Harris, 2012). A two-  
163 factor solution of the TSK-11 version provides the best fit in terms of explaining variance across  
164 German, Dutch, Swedish and Canadian samples and included the subscales “activity-avoidance”  
165 (TSK-AA, the belief that that activity may result in (re)injury or stronger pain) and “somatic  
166 focus” (TSK-SF, the belief in underlying and serious medical problems) (Roelofs et al., 2007;  
167 Rusu et al., 2014).

168 (2) The German version of the fear avoidance beliefs questionnaire (FABQ) (Waddell et al.,  
169 1993; Pfingsten et al., 2000) consists of 16 back pain-specific items related to fear avoidance  
170 beliefs rated on a 7-point rating scale (0 = “completely disagree” to 6 = “completely agree”). It  
171 includes two distinct and established subscales related to beliefs about on how work (FABQ-W)  
172 and physical activity (FABQ-PA) affects LBP with internal consistencies of  $\alpha = 0.88$  and  $\alpha =$   
173  $0.77$ , respectively (Waddell et al., 1993).

174 (3) The short version of the Pain Anxiety Symptoms Scale (PASS-20) assesses fear and anxiety  
175 responses related to pain including cognitive, physiological and motor response domains  
176 (McCracken and Dhingra, 2002). Items on the PASS-20 are measured on a 6-point Likert scale  
177 and relate to four different subscales including cognitive anxiety (PASS-C), fear (PASS-F),  
178 physiology (PASS-P) and escape/avoidance (PASS-E) (Roelofs et al., 2004b). The German  
179 version of the PASS-20 has an internal consistency of  $\alpha = 0.90$  (Kreddig et al., 2015).

180 Furthermore, patients were asked to fill out the painDETECT (PD-Q) questionnaire that includes  
181 three 11-point numeric rating scales (NRS), with 0 being “no pain” and 10 being the “worst  
182 imaginable pain” to assess current pain, strongest and average pain intensity in the previous 4  
183 weeks (Freyenhagen et al., 2006). Finally, to investigate potential differences or shared variance  
184 between PRF and general anxiety, we used the State-Trait Anxiety Inventory (STAI), the most  
185 widely used self-report measure of anxiety which includes two subscales (Spielberger and  
186 Gorsuch, 1983; Julian, 2011): The State Anxiety Scale (S-Anxiety) assesses current levels of  
187 anxiety whereas the Trait Anxiety Scale (T-Anxiety) evaluates more stable aspects of anxiety  
188 such as “anxiety proneness” (Julian, 2011). All questionnaires were administered at the fMRI  
189 appointment prior to brain scanning. We tested the scores of the different questionnaires for the  
190 assumption of normality of the data using the Shapiro-Wilk test and visually using Q-Q plots  
191 implemented in IBM SPSS Statistics (version 23) (Ghasemi and Zahediasl, 2012).

### 192 **2.3 Scanning protocol and design**

193 Brain imaging was performed on a 3-T whole-body MRI system (Philips Achieva, Best,  
194 Netherlands), equipped with a 32-element receiving head coil and MultiTransmit parallel RF  
195 transmission. Each imaging session started with a survey scan, a B1 calibration scan (for  
196 MultiTransmit), and a SENSE reference scan. High resolution anatomical data were obtained  
197 with a 3D T1-weighted turbo field echo scan consisting of 145 slices in sagittal orientation with  
198 the following parameters: FOV =  $230 \times 226 \text{ mm}^2$ ; slice thickness = 1.2 mm; acquisition matrix =  
199  $208 \times 203$  (resulting in a voxel resolution of 1.1mm x 1.1mm x 1.2mm); TR = 6.8 ms; TE = 3.1  
200 ms; flip angle =  $9^\circ$ ; number of signal averages = 1. Functional time series were acquired using  
201 whole-brain gradient-echo echo planar imaging (EPI) sequences (365 volumes), consisting of 37  
202 slices in the axial direction (AC-PC angulation) with the following parameters: field of view

203 (FOV) =  $240 \times 240 \text{ mm}^2$ ; acquisition matrix =  $96 \times 96$ ; slice thickness = 2.8 mm (resulting in a  
204 voxel resolution of 2.5mm x 2.5mm x 2.8mm); interleaved slice acquisition; no slice gap;  
205 repetition time (TR) = 2100 ms; echo time (TE) = 30 ms; SENSE factor = 2.5; flip angle  $80^\circ$ .

206 The PRF-provoking stimuli (harmful condition) consisted of video clips with a duration of 4 s  
207 recorded from a 3rd person perspective (Meier et al., 2016). The video clips showed potentially  
208 harmful activities (back straining movements such as bending and lifting) selected from the  
209 Photograph Series of Daily Activities (PHODA) (Leeuw et al., 2007a). The original PHODA  
210 was developed in close collaboration with human movement scientists, physical therapists, and  
211 psychologists and is comprised of a fear hierarchy based on ratings of perceived harmfulness of  
212 daily activities in patients with chronic LBP. From the 40 potentially harmful activities included  
213 in the short electronic PHODA version (Leeuw et al., 2007a), we chose three scenarios from the  
214 top six most harmful activities, namely shoveling soil with a bent back, lifting a flowerpot with  
215 slightly bent back and vacuum cleaning under a coffee table with a bent back. Furthermore, we  
216 created video clips of three activities rated as less harmful, such as walking up and down the  
217 stairs and walking on even ground (harmless condition). Presentation® software  
218 (Neurobehavioral Systems, Davis, CA, USA) was used to present the video clips in a pseudo-  
219 randomized order (no more than two identical consecutive trials). The patients were asked to  
220 carefully observe the video clips which were displayed using MR-compatible goggles  
221 (Resonance Technology, Northridge, CA, USA). The three harmful and harmless activities were  
222 each presented five times (30 trials total). After the observation of each video clip, the patients  
223 were asked to rate the perceived harmfulness of the activity on a visual analog scale (VAS)  
224 anchored with the endpoints “not harmful at all” (0) and “extremely harmful” (10). All ratings  
225 were performed using a MR compatible track ball (Current Designs, Philadelphia, PA, USA).

226 After the VAS rating, a black screen with a green fixation cross appeared (duration jittered  
227 between 6s and 8s). We have used this experimental protocol successfully for investigations of  
228 neural correlates of PRF self-reports in previous fMRI studies based on mass-univariate analyses  
229 (Meier et al., 2016; Meier et al., 2017).

#### 230 **2.4 MR data organization and pre-processing**

231 We used an existing fMRI dataset of previously reported studies (Meier et al., 2016; Meier et al.,  
232 2017). The fMRI data were organized according to the Brain Imaging Data Structure (BIDS,  
233 RRID: SCR\_016124, <http://bids.neuroimaging.io/>), which provides a consensus on how to  
234 organize data obtained in neuroimaging experiments. Preprocessing was performed using  
235 FMRIprep (version 1.0.0-rc2, , RRID:SCR\_016216, <https://github.com/poldracklab/fmriprep>),  
236 a Nipype based tool (Gorgolewski et al., 2011), which requires minimal user input and provides  
237 easily interpretable and comprehensive error and output reporting. This processing pipeline  
238 includes state-of-the-art software packages for each step of pre-processing (see  
239 <https://fmriprep.readthedocs.io/en/stable/workflows.html> for a detailed description of the  
240 different workflows). Each T1-weighted (T1w) volume was skullstripped using  
241 `antsBrainExtraction.sh v2.1.0` (using OASIS template). The skullstripped T1w volume was co-  
242 registered to the skullstripped ICBM 152 Nonlinear Asymmetrical MNI template version 2009c  
243 using nonlinear transformation implemented in ANTs v2.1.0 (Avants et al., 2008). Functional  
244 data were slice time corrected using AFNI (Cox, 1996) and motion corrected using MCFLIRT  
245 v5.0.9 (Jenkinson et al., 2002). This was followed by co-registration to the corresponding T1w  
246 volume using boundary based registration 9 degrees of freedom - implemented in FreeSurfer  
247 v6.0.0 (Greve and Fischl, 2009). Motion correcting transformations, T1w transformation and  
248 MNI template warp were applied in a single step using `antsApplyTransformations v2.1.0` with

249 Lanczos interpolation. Three tissue classes were extracted from T1w images using FSL FAST  
250 v5.0.9 (Zhang et al., 2001). Voxels from cerebrospinal fluid and white matter were used to create  
251 a mask used to extract physiological noise regressors using aCompCor (Behzadi et al., 2007).  
252 The mask was eroded and limited to subcortical regions to limit overlap with grey matter and six  
253 principal components were estimated. Independent component analysis (ICA)-based Automatic  
254 Removal Of Motion Artifacts (AROMA) was used to generate aggressive motion-related noise  
255 regressors. The AROMA classifier identifies motion components with high accuracy and  
256 robustness and is superior to motion artefact detection using 24 motion parameters or spike  
257 regression (Pruim et al., 2015). Finally, to preserve high spatial frequency while reducing noise,  
258 spatial smoothing with a full width at half maximum 4mm Gaussian kernel was applied. To  
259 accelerate data pre-processing we performed parallel computing using the Docker environment  
260 (<https://www.docker.com/>) and the GC3Pie framework (<https://github.com/uzh/gc3pie>) on the  
261 ScienceCloud supercomputing environment at the University of Zurich (S3IT,  
262 <https://www.s3it.uzh.ch/>).

### 263 **2.5 MVPA input data**

264 The pre-processed data were subsequently passed onto Statistical Parametric Mapping software  
265 package (SPM12, version 6906, RRID: SCR\_007037, <http://www.fil.ion.ucl.ac.uk/spm/>) for  
266 model computation using a general linear model (GLM). For each patient a design matrix was  
267 built with separate regressors for the harmful and harmless activities, respectively (15 harmful  
268 and 15 harmless stimuli). The video clips were modeled as boxcar functions (onset=onset of  
269 video clip; duration=4s) and convolved with the standard canonical hemodynamic response  
270 function (HRF) as implemented in SPM12. In addition, the following nuisance regressors were  
271 implemented in the GLM model for each patient: (1) the six regressors derived from the

272 component based physiological noise correction method (aCompCor) and (2) the motion-related  
273 regressors generated by AROMA (see section 2.4). A high-pass filter with a cut-off of 128 s was  
274 used to remove low-frequency noise. Finally, for each patient, voxel-wise beta images for each  
275 condition were computed and served as the input images for the MVPA.

## 276 **2.6 Multivariate pattern analysis (MVPA)**

277 Compared to univariate analyses, MVPA can achieve greater sensitivity and is able to detect  
278 subtle and spatially distributed effects (Schrouff et al., 2013; Haynes, 2015). A pattern of activity  
279 can represent many more different states than each voxel individually, which leads to an  
280 information-based view compared to the activation-based view of univariate analyses (Hebart  
281 and Baker, 2017). MVPA was performed using routines implemented in PRoNTo v.2.0 (RRID:  
282 SCR\_006908, <http://www.mnl.cs.ucl.ac.uk/pronto/>) (Schrouff et al., 2013). For the read-out of  
283 multivariate neural information that might serve as a potential score estimator of the different  
284 PRF questionnaires, we applied a newly introduced pattern regression approach based on  
285 supervised machine learning and testing phases using Multiple Kernel Learning (MKL). In brief,  
286 the objective in supervised pattern recognition regression analysis is to learn a function from data  
287 that can accurately predict the continuous values (labels), i.e.  $f(x_i)=y_i$  from a given dataset  $D=\{x_i,$   
288  $y_i\}$ ,  $i=1\dots N$  where  $x_i$  represents pairs of samples or vectors and  $y_i$  the different labels. Ultimately,  
289 the learned function from the learning set is used to predict the labels from new and unseen data  
290 (Schrouff et al., 2013). MKL allows to account for brain anatomy (determined by a brain atlas,  
291 see section 2.7) and different modalities (such as anatomical/functional data or in the current  
292 approach: conditions) during the model estimation by considering each brain region and  
293 modality as separate kernels. This approach allows determining the contribution of each brain  
294 region (region weights) and condition (condition weights) to the final decision function of the

295 model in a hierarchical manner by simultaneously learning and combining the different linear  
296 kernels that are based on support vector machines (SVM) (Rakotomamonjy et al., 2008;  
297 Fernandes et al., 2017; Schrouff et al., 2018). Compared to conventional MVPA methods based  
298 on whole-brain voxel weight maps, this procedure provides a straight-forward approach to draw  
299 inferences on the region level without the need for multiple comparison correction (Schrouff et  
300 al., 2018). To account for possible differential contributions of the harmful and harmless  
301 conditions to the decision function, we included the individual SPM beta images of each  
302 condition as separate modalities in the MKL model (condition weights). The kernels were mean  
303 centered and normalized (to account for the different sizes of the involved brain regions) using  
304 standard routines implemented in PRoNTo. Subsequently, for each questionnaire, we trained a  
305 separate MKL regression model with the respective labels (FABQ, TSK-17-, -13- and -11-item,  
306 PASS and all subscale scores, state and trait anxiety). Furthermore, we trained MKL regression  
307 models based on the harmfulness ratings collected during the fMRI measurements (mean ratings  
308 of the harmful condition and harmless condition, respectively). This resulted in a total of 17  
309 MKL models providing outputs for model evaluation, including model performance, region and  
310 conditions weights. To reduce the risk of overfitting for each model, we applied a nested cross-  
311 validation procedure using a “leave-one-subject-out” cross-validation scheme to train the model  
312 including optimization of the model's hyperparameter “C” (range [0.1 1 10 100 1000]).  
313 Furthermore, to generate a data-based null distribution of the performance measures (r and  
314 nMSE, see section 2.8), each model was re-computed 16'000 times with permuted labels  
315 (permuted questionnaire score per subject) using parallel computing. Multiple comparison  
316 correction for the model performance (r's and nMSE) was based on a false discovery rate (FDR)  
317 of 5% ( $p(\text{FDR}) < 0.05$ ). As a note, by controlling the expected proportion of false-positives,

318 FDR-controlling procedures provide less stringent control of Type I errors compared to other  
319 procedures such as Bonferroni correction, which control the probability of at least one Type I  
320 error. In addition, each model representing a potential PRF construct, i.e. a model with a  
321 significant (FDR corrected and uncorrected) performance, was trained and tested through an  
322 additional cross-validation procedure using each predictive feature set (brain regions that  
323 contributed >10%, see Table 4) of the other models (between-model cross-validation, e.g.  
324 training and testing of the FABQ labels was repeated using the predictive feature sets of the  
325 TSK-11, TSK-13 and T-Anxiety models). A failure of predictive performance in the between-  
326 model cross-validation would point towards a dissociation of brain regions contributing to the  
327 different models and would therefore be indicative of non-overlapping PRF constructs.

## 328 **2.7 Feature selection**

329 To further reduce the risk of overfitting and based on a-priori knowledge of brain regions  
330 involved in fear processing, we limited the feature space to bilateral fear-related brain regions  
331 including the amygdala, hippocampus, thalamus, anterior cingulate, insula, medial prefrontal and  
332 orbitofrontal cortices (Tovote et al., 2015; Braem et al., 2017; Meier et al., 2014). The respective  
333 brain regions were parcellated according to the Automated Anatomical Labeling (AAL, RRID:  
334 SCR\_003550, <http://qnl.bu.edu/obart/explore/AAL/>, see Table 4 for the different labels)  
335 (Tzourio-Mazoyer et al., 2002) atlas and projected on the ICBM 152 Nonlinear template (section  
336 2.4) by means of MATLAB (version R2017b) based surface-volume registration tools (svreg)  
337 implemented in BrainSuite (version 17a, RRID: SCR\_006623, <http://brainsuite.org/>) (Shattuck  
338 and Leahy, 2002). BrainSuite was also used to generate surfaces of the selected AAL regions for  
339 visualization.

## 340 **2.8 Model evaluation and interpretation**

341 Model performance was assessed by two metrics commonly used to assess the performance of  
342 regression models (Ivanescu et al., 2016; Fernandes et al., 2017): Pearson's correlation  
343 coefficient ( $r$ ) and the mean squared error (MSE). The correlation coefficient characterizes the  
344 linear relationship between observed and predicted labels; the MSE is calculated as the average  
345 of the squared differences between the observed and predicted labels. A significant positive  
346 correlation between observed and predicted labels would indicate strong decoding performance.  
347 Unlike in conventional correlation analysis, however, a negative correlation would indicate poor  
348 performance. Furthermore, for each model, we report the normalized MSE (nMSE) because the  
349 different questionnaires are based on different score ranges. To explore possible differential  
350 contributions of fear-related brain regions to the prediction models, we report the contribution  
351 rank of each brain region (region weight) within each condition (condition weight) provided by  
352 the MKL approach (Table 4). Importantly, the selection of regions by the MKL model might be  
353 influenced by small variations in the dataset (because of the leave-one-subject-out cross-  
354 validation) and might therefore lead to different subsets of regions being selected across cross-  
355 validation steps (folds). Providing a quantification of this variability, the "expected ranking  
356 (ER)" (see Table 4) characterizes the stability of the region ranking across folds: The closer the  
357 ER to the ranking of the selected fold, the more consistent is the ranking of the respective brain  
358 region across folds. On the other hand, if the ER is different from the ranking, this means that the  
359 ranking might be variable across folds.

## 360 **3. Results**

### 361 **3.1 Ratings, questionnaire scores and correlations**

362 Importantly, the comparison of the ratings during fMRI measurements demonstrated that the  
363 potentially harmful activities were perceived as being significantly more harmful compared to  
364 the harmless activities (paired-T-Test:  $T = 8.22$ ,  $p < 0.001$ , two-tailed). Descriptive statistics of  
365 the different questionnaires as well as age and sex of the patients are summarized in Table 1.  
366 Regarding the questionnaire data, visual inspection (Q-Q plots) and the Shapiro-Wilk test  
367 indicated non-normality of the data ( $p < 0.05$ ) of several questionnaires (FABQ, FABQ-W, TSK-  
368 11, FABQ-PA and T-Anxiety) and therefore, the non-parametric Spearman's rank correlation  
369 coefficient was used. Several significant positive correlations between the different PRF  
370 questionnaires scores were observed ( $p < 0.05$ , Table 2). Most of the TSK scales significantly  
371 correlated with the PASS scales ( $0.97 < r's > 0.46$ ,  $p < 0.05$ ) whereas the FABQ work scale did  
372 not show significant relationships with the TSK and PASS scales ( $p > 0.05$ ), except for the  
373 PASS-F scale ( $r = 0.49$ ,  $p < 0.05$ ). Furthermore, only the S-Anxiety scale of the STAI scale  
374 demonstrated significant correlations with some, but not all, TSK scales ( $0.44 < r's > 0.63$ ,  $p <$   
375  $0.05$ ). Finally, only the PASS-F scale showed a positive and significant relationship with the  
376 mean rating of the harmful condition ( $r = 0.44$ ,  $p < 0.05$ , Table 2).

### 377 **3.2 Model performance**

378 The MKL models with significant performance results ( $p < 0.05$ , FDR- and uncorrected)  
379 characterized by the Pearson's correlation coefficient ( $r$ ) and the normalized mean squared error  
380 (nMSE) are depicted in Figure 1 (A-E, see also Table 3A for results overview). The FABQ  
381 model demonstrated a significant decoding performance characterized by a positive correlation  
382 between true and predicted labels ( $r = 0.61$ ,  $p(\text{FDR}) = 0.012$ ,  $\text{nMSE} = 4.25$ ,  $p(\text{uncorr}) = 0.014$ ).  
383 Interestingly, the FABQ-W model showed strong predictive power ( $r = 0.74$ ,  $p(\text{FDR}) = 0.004$ ,  
384  $\text{nMSE} = 1.81$ ,  $p(\text{FDR}) = 0.003$ ) whereas the FABQ-PA scale was not decodable from fear-

385 related brain response patterns ( $r = 0.03$ ,  $p(\text{uncorr}) = 0.162$ ,  $n\text{MSE} = 1.68$ ,  $p(\text{uncorr}) = 0.161$ ).  
386 Among the TSK scales, only the TSK-13- ( $r = 0.37$ ,  $p(\text{uncorr}) = 0.034$ ,  $n\text{MSE} = 1.09$ ,  $p(\text{uncorr})$   
387  $= 0.033$ ) and the TSK-11- ( $r = 0.63$ ,  $p(\text{FDR}) = 0.009$ ,  $n\text{MSE} = 0.90$ ,  $p(\text{uncorr}) = 0.032$ ) models  
388 demonstrated a significant decoding performance. The TSK-17 model ( $r = 0.19$ ,  $p(\text{uncorr}) =$   
389  $0.09$ ,  $n\text{MSE} = 1.10$ ,  $p(\text{uncorr}) = 0.091$ ) and the TSK-11 subscale models did not show a  
390 significant decoding performance (TSK11-SF: ( $r = -0.73$ ,  $p(\text{uncorr}) = 0.832$ ,  $n\text{MSE} = 0.86$ ,  
391  $p(\text{uncorr}) = 0.773$  / TSK-11-AA:  $r = -0.63$ ,  $p(\text{uncorr}) = 0.908$ ,  $n\text{MSE} = 0.88$ ,  $p(\text{uncorr}) = 0.879$ ).  
392 In addition, none of the PASS scales were decodable from fear-related brain response patterns  
393 (PASS:  $r = 0.18$ ,  $p(\text{uncorr}) = 0.119$ ,  $n\text{MSE} = 4.63$ ,  $p(\text{uncorr}) = 0.115$  / PASS-C:  $r = -0.44$ ,  
394  $p(\text{uncorr}) = 0.515$ ,  $n\text{MSE} = 1.64$ ,  $p(\text{uncorr}) = 0.513$  / PASS-E:  $r = -0.32$ ,  $p(\text{uncorr}) = 0.339$ ,  
395  $n\text{MSE} = 1.38$ ,  $p(\text{uncorr}) = 0.331$ , PASS-F:  $r = -0.15$ ,  $p(\text{uncorr}) = 0.259$ ,  $n\text{MSE} = 1.70$ ,  $p(\text{uncorr})$   
396  $= 0.251$  / PASS-P:  $r = -0.51$ ,  $p(\text{uncorr}) = 0.518$ ,  $n\text{MSE} = 1.36$ ,  $p(\text{uncorr}) = 0.512$ ). Furthermore,  
397 the T-Anxiety model demonstrated a moderate decoding performance ( $r = 0.48$ ,  $p(\text{FDR}) = 0.011$ ,  
398  $n\text{MSE} = 1.01$ ,  $p(\text{uncorr}) = 0.015$ ) whereas the S-Anxiety model was not significant ( $r = -0.46$ ,  
399  $p(\text{uncorr}) = 0.481$ ,  $n\text{MSE} = 1.51$ ,  $p(\text{uncorr}) = 0.475$ ). The ratings of perceived harmfulness  
400 during fMRI measurements were not decodable from fear-related brain response patterns (Rating  
401 harmful:  $r = -0.01$ ,  $p(\text{uncorr}) = 0.247$ ,  $n\text{MSE} = 0.64$ ,  $p(\text{uncorr}) = 0.242$  / Rating harmless:  $r = -$   
402  $0.72$ ,  $p(\text{uncorr}) = 0.481$ ,  $n\text{MSE} = 0.38$ ,  $p(\text{uncorr}) = 0.441$ ). Finally, the between model cross-  
403 validation (see section 2.6) did not result in significant performance results ( $p(\text{uncorr}) > 0.11$ )  
404 between different feature sets (e.g. FABQ labels were not predictable using the TSK-11 feature  
405 set, Table 3B).

### 406 3.3 Condition and region weights

407 The condition and region weights of models with predictive performance ( $p < 0.05$ , FDR- and  
408 uncorrected, section 3.2) are illustrated in Figure 1 (A-E) and described in detail in Table 4 (A-  
409 E). The decoding performances of the FABQ models (FABQ and FABQ-W) were driven by a  
410 major contribution of the harmful condition (88% and 87%, respectively). Within this condition,  
411 the left thalamus (rank 1), the right amygdala (rank 2) and the left hippocampus (rank 3)  
412 contributed more than 69% of the total region weights in the FABQ model (Table 4A, Figure  
413 3A). Similarly, the right amygdala (rank 1) and the left thalamus (rank 2) carried the most  
414 predictive neural information with 79,42% of the total region weights in the FABQ-W model  
415 (Table 4B, Figure 3B). In both FABQ models, the right amygdala also demonstrated an  
416 association with the harmless condition, although of minor relevance (~11%). In comparison, the  
417 TSK models demonstrated a moderate contribution of the harmful condition (TSK-13:60%,  
418 TSK-11:66%). Both predictive model performances of the TSK were driven by a major  
419 contribution of the right lateral orbitofrontal cortex (lOFC, TSK-13: 52.7%, TSK-11: 60,49%,  
420 Table 4C,D, Figure 3C,D). Furthermore, the left medial orbitofrontal cortex (mOFC) and the  
421 right hippocampus carried predictive information within the harmless condition in both TSK  
422 models (TSK-13: left gyrus rectus 19.51%, right hippocampus: 14.03% / TSK-11: left gyrus  
423 rectus: 21.29%, right hippocampus: 10.41%). With almost equal contributions of the harmful  
424 (52%) and harmless conditions (48%), the prediction of the T-Anxiety scores was mainly driven  
425 by neural contributions of the left medial prefrontal (mPFC) and mOFC (accounting for 44% of  
426 the total region weights in the harmful condition) and the left thalamus (together with the mOFC  
427 accounting for 44% of the total region weights in the harmless condition, Table 4E, Figure 3E).

#### 428 **4. Discussion**

429 Evidence from cross-sectional and longitudinal behavioral studies demonstrates a strong  
430 association between PRF and disability in chronic pain (Leeuw et al., 2007b; Esteve et al., 2017;  
431 Wertli et al., 2014b). However, the different PRF constructs such as “fear of  
432 movement/(re)injury/kinesiophobia”, “fear avoidance beliefs” or “pain anxiety” are often used  
433 interchangeably in the literature (Lundberg et al., 2011) and it is unclear if they share a common  
434 PRF construct reflected by similar neural sources. The (sub-)cortical neural basis of fear and  
435 anxiety that controls cognitions and regulates appropriate behavior dependent on threat  
436 characteristics is well described (Gray and MacNaughton, 2000; McNaughton and Corr, 2004;  
437 Qi et al., 2018; Shackman et al., 2011; Panksepp, 2011; LeDoux, 2000). Although both emotions  
438 are linked to similar neuromodulatory systems of the fear circuit (Tovote et al., 2015), anxiety is  
439 less well understood and more complex than fear. Current research suggests a functional  
440 differentiation characterized by subcortical regions processing fast fear responses to an imminent  
441 threat (defensive responses) and cortical systems processing complex cognitions related to fear  
442 and anxiety where the threat is distal in space or time (Qi et al., 2018; LeDoux and Pine, 2016).

443 The current MVPA approach using MKL demonstrated the feasibility to neuronally dissect the  
444 proposed constructs of PRF self-reports based on their (sub-)cortical predictors during PRF  
445 related brain activity. The results revealed that while the variability across individuals of some  
446 questionnaires, specifically the FABQ- and FABQ-W-, TSK-13, TSK-11 and T-Anxiety-scale,  
447 was predictable from response patterns in fear-related, dissociable neural sources on subcortical  
448 and cortical levels, this was not the case for the FABQ-PA-, the TSK-11 subscales (TSK-11-AA  
449 and TSK-SF), the PASS scales and the S-Anxiety scale. Furthermore, the online ratings of  
450 perceived harmfulness were not decodable from fear-related brain response patterns.

451 *FABQ and TSK*

452 The FABQ and FABQ-W scales demonstrated the best model performances among the  
453 investigated PRF questionnaires, characterized by a strong contribution of neural information in  
454 the harmful condition (condition weights: 88% and 87%, respectively). Interestingly, the FABQ-  
455 PA scale did not show a predictive association with fear-related brain response patterns. The  
456 better model performance of the FABQ-W based on fear-related brain activity patterns is in line  
457 with the emerging evidence that the FABQ-W is a better predictor of treatment outcome in  
458 chronic LBP compared to the FABQ-PA, although this might be dependent on the patient  
459 population (George et al., 2005; George et al., 2008; Waddell et al., 1993; Wertli et al., 2014a).  
460 In support of this, the FABQ-W scale qualified for a clinical prediction rule regarding  
461 improvement after spinal manipulation, whereas the FABQ-PA scale did not (Dougherty et al.,  
462 2014; Flynn et al., 2002).

463 With respect to the region weights, the FABQ models were mainly driven by subcortical neural  
464 contributions involving the thalamus, hippocampus and the amygdala while frontal brain regions  
465 played a minor role. The thalamus and particularly its midline structures have been considered to  
466 be a non-specific arousing system (van der Werf et al., 2002). However, it has been recently  
467 shown that parts of dorsal midline thalamic structures are necessary for fear memory processing  
468 by directly targeting the hippocampus, which plays an important role for context-dependent  
469 emotional memory (Penzo et al., 2015; Lara-Vásquez et al., 2016; Zheng et al., 2017).  
470 Furthermore, the amygdala has long been considered a “fear center” (Panksepp, 1998; Darwin,  
471 1873). However, the heterogeneous structure consisting of several nuclei is not essential for the  
472 *experience* of fear, demonstrated in patients with amygdala lesions (Anderson and Phelps, 2002;  
473 Feinstein et al., 2013; LeDoux and Pine, 2016). Instead, the amygdala has been shown to be  
474 more strongly implicated in behavioral and physiological responses to threats (i.e. defensive

475 processes); its relation to complex cognitions like fear and anxiety is controversial (Fanselow  
476 and Pennington, 2017; LeDoux and Pine, 2016; Panksepp, 2011). A recent opinion paper  
477 suggests that subjective feelings of fear and anxiety do not initially arise from subcortical activity  
478 of the fear circuit centered around the amygdala (LeDoux and Hofmann, 2018). Thus, amygdala  
479 activity and mediated physiological responses of fear and anxiety might be, at its best, only a  
480 correlate of subjective feelings of fear and anxiety (LeDoux and Hofmann, 2018). Nevertheless,  
481 the results presented here indicate a strong predictive association between subjective reports of  
482 PRF, assessed by the FABQ scales, and amygdala activity patterns.

483 Among the TSK scales, the TSK-13 and the TSK-11 demonstrated a predictive association with  
484 fear-related brain response patterns, albeit with less contribution of the harmful condition  
485 compared to the FABQ scales (TSK-13: 60% and TSK-11: 66%). The TSK-11 version showed a  
486 stronger relationship between true and predicted labels compared to the TSK-13 version ( $r =$   
487  $0.60$ ,  $nMSE = 0.90$ ,  $p < 0.05$ ). This result might reflect the progress of previous research  
488 regarding the psychometric properties of the different TSK versions. Compared to the 17-item  
489 version, the 13-item version has better psychometric properties without the four inversely  
490 phrased items (Roelofs et al., 2004a; Neblett et al., 2016) and the 11-item version has been  
491 recommended for future research and clinical settings (for a chronological summary see Tkachuk  
492 and Harris, 2012). Interestingly, no predictive association could be “learned” by MKL using the  
493 TSK-11 subscale labels (TSK-11-SF and TSK-11-AA scores). Although these two lower order  
494 factors (activity avoidance and somatic focus) are reflective of the higher order construct “fear of  
495 movement and (re)injury/kinesiophobia”, the non-significant result might indicate that they are  
496 associated with inconsistent neural patterns across individuals.

497 Regarding the region weights of the TSK models, the right lateral orbitofrontal cortex (IOFC)  
498 provided the most predictive information for the two TSK scales (TSK-13: 52%, TSK-11: 60%).  
499 In agreement with the phobia-related construct (kinesiophobia), dysfunction of the OFC has been  
500 shown to be implicated in the processing of phobia-related stimuli in disorders such as social  
501 anxiety disorder (Dilger et al., 2003). Specifically, IOFC activity was reduced when phobogenic  
502 trials were contrasted with fear-relevant trials (Aue et al., 2015). Furthermore, a hyperactive  
503 IOFC has been shown to be linked to anxiety-laden cognitions (Hahn et al., 2011). Interestingly,  
504 the higher cortical contributions of the TSK models were clearly dissociable from the largely  
505 subcortical contributions involving the amygdala, hippocampus and thalamus that predicted the  
506 FABQ scores.

507 To conclude, the FABQ scales demonstrated high PRF sensitivity (harmful condition weights >  
508 87%) and were linked to subcortical predictors that have been associated with fear responses to  
509 an imminent threat and defensive behavior (LeDoux and Pine, 2016; McNaughton and Corr,  
510 2004). In contrast, the TSK scales appeared to capture emotional states largely associated with  
511 cortical fear processing that might be related to cognitive aspects of PRF. In support of this, the  
512 observed higher harm/less condition weights of the TSK compared to the FABQ models might  
513 indicate that the TSK scales are associated with more diffuse anxiety-related cognitions.

514 *PASS*

515 Surprisingly, the PASS failed to demonstrate a predictive association with fear-related brain  
516 response patterns. There may be several explanations. First, whereas the FABQ and the TSK  
517 scales have been specifically developed for patients with musculoskeletal pain, the PASS is  
518 suitable for various pain phenotypes (Crombez et al., 1999). Second, the PASS has been shown  
519 to be more strongly associated with negative affect and less predictive of pain disability and

520 behavioral performance (Crombez et al., 1999). Third, all PASS subscales demonstrated  
521 significant multicollinearity in our sample suggesting non-independence between the different  
522 subscales. All these aspects may have led to less sensitivity of fear related neural patterns to the  
523 PASS and its subscales in the current study.

524 The superiority of the FABQ scale (driven by the FABQ-W) in decoding performance compared  
525 to the TSK and PASS scales might also be influenced by the back-specific items of the FABQ in  
526 conjunction with the nature of the PRF-provoking stimuli (back straining movements). The items  
527 of the FABQ were specifically related to the back while the TSK and PASS can be used with  
528 various musculoskeletal pain diagnoses such as work-related upper extremity disorders, chronic  
529 LBP, fibromyalgia, and osteoarthritis (Roelofs et al., 2007). Nevertheless, the FABQ has also  
530 been adapted to shoulder pain where it demonstrated better factor structure and a stronger  
531 association with disability compared to the TSK-11 (Mintken et al., 2010).

### 532 *State and Trait anxiety*

533 Beside PRF, anxiety and depression significantly mediate the relationship between pain and  
534 disability (Marshall et al., 2017). Nevertheless, fear responses specifically related to a patient's  
535 pain and/or potentially painful movements might be more relevant for explaining disability in  
536 chronic LBP than general trait anxiety responses (McCracken et al., 1996). The current results  
537 are in line with this notion. First, most of the PRF measures did not show a significant  
538 relationship with state or trait anxiety. Second, state anxiety was not decodable from fear-related  
539 brain responses to potentially harmful activities in chronic pain patients. Interestingly, with  
540 respect to the trait anxiety model (T-Anxiety, Figure 1E), the harmful and the harmless  
541 conditions carried almost equal predictive neural information (52% vs. 48%). This suggests that  
542 the trait anxiety measure is associated with neural content irrespective of the harmfulness of a

543 stimulus, provoked by e.g. enhanced attention to visual information processed in fear-related  
544 brain regions (Berggren et al., 2015). It might further indicate that the T-Anxiety scale captures  
545 neural responses that are associated with a more generalized fear response.

546 Regarding the region weights, predictive information was predominantly provided by brain  
547 regions that were less involved in the prediction of the other PRF measures, namely parts of the  
548 mPFC and mOFC (Table 4E). This is in line with the proposed functional differentiation of  
549 neural structures regarding fear in response to an imminent threat (defensive response) and  
550 cognitive fear/anxiety (distal, uncertain threat) whereas the latter involves more rostral cortical  
551 structures such as the mPFC and mOFC (LeDoux and Pine, 2016; McNaughton and Corr, 2004).  
552 Moreover, research on self-report measurements indicates that trait anxiety is relatively distinct  
553 from tissue damage fear, which supports a behavioral and neural dissociation of trait anxiety and  
554 PRF (Perkins et al., 2007; Cooper et al., 2007).

#### 555 *Harmfulness ratings*

556 Interestingly, although the PRF-provoking harmful activities were rated as significantly more  
557 harmful compared to the harmless activities, the ratings of perceived harmfulness during fMRI  
558 measurements were not decodable from fear-related brain response patterns. Furthermore, the  
559 ratings did not show significant correlations with PRF measures (except the PASS-F scale, see  
560 Table 2). Others reported only moderate relationships ( $r$ 's < 0.39) between perceived  
561 harmfulness ratings of PHODA items and self-report measures such as the TSK, Pain  
562 Catastrophizing scale (PCS) or pain intensity (Leeuw et al., 2007a), indicating that ratings of  
563 perceived harmfulness assess something akin to, but also distinct from PRF self-report measures.  
564 The weak relationships between ratings of perceived harmfulness and self-report measures of  
565 PRF might be explained by the specificity of the potentially harmful movements depicted by the

566 PHODA items. Namely, the ratings of perceived harmfulness were specifically related to back  
567 straining movements such as bending and lifting while the PRF measures might also be  
568 associated with other potentially harmful movements. As such, the fear-related neural patterns  
569 induced by the observation of potentially harmful activities for the back might not include  
570 information about movement specificity. Instead, these neural patterns might predict PRF and its  
571 constructs in a more general fashion that is captured by the TSK and FABQ.

#### 572 *Limitations*

573 A limitation of this study is the relatively small sample size in conjunction with the cross-  
574 validation framework. Ideally, the predictive model should be trained and tested with completely  
575 independent data. However, the results obtained are likely to be valid for several reasons: 1) the  
576 goal of the current study was not maximizing decoding performance, rather, multivariate  
577 decoding was used for the interpretation and understanding of the different PRF constructs, for  
578 which significant predictive accuracy was obtained (Hebart and Baker, 2017); 2) the applied  
579 linear SVM has been shown to exhibit good performance even in very high dimensional settings  
580 with small sample sizes (Varoquaux and Thirion, 2014); 3) the applied regression approach using  
581 continuous variables enhances statistical power compared to a categorical analysis (e.g. low  
582 versus high fear) (Altman and Royston, 2006); 4) the variability of the regions most contributing  
583 to the models across cross-validation folds was very small (indicated by the expected ranking  
584 (ER)), demonstrating stable ranking, irrespective of which subject's data were left out for  
585 validation. For these reasons, the differences of the prediction models are unlikely to be caused  
586 by the small sample size. A further limitation is related to the sparsity approach (L1  
587 regularization) of the MKL algorithm currently implemented in PRoNT which does not select  
588 brain regions with highly correlated neural information. Therefore, potential lateralization effects

589 of brain regions (e.g. left and right amygdala) should be carefully interpreted. Finally, the study  
590 design only allows interpretations of PRF to back straining movements and LBP. Therefore,  
591 conclusions related to other musculoskeletal conditions should be drawn with caution.  
592 Nevertheless, the current approach might represent a promising new tool to dissect psychological  
593 constructs of self-report measures by using their neural predictors.

#### 594 *Conclusion*

595 This is the first time that multivariate brain responses patterns are used to better understand and  
596 dissect a psychological construct, here, PRF, conventionally assessed by self-report  
597 (questionnaires). Relating content-selective neural information to potentially different  
598 psychological constructs likely supports their construct validity by revealing (hidden)  
599 commonalities or differences across psychological constructs. Indeed, dissociable fear-related  
600 neural information served as score estimators of the FABQ (FABQ total and FABQ-W), the TSK  
601 (13- and 11-item versions), and the T-Anxiety questionnaire, supporting the distinctness of the  
602 fear constructs behind these questionnaires. The FABQ scales demonstrated strong predictive  
603 power with high sensitivity to the harmful condition and were associated with subcortical fear  
604 processing regions (amygdala, thalamus, hippocampus). The TSK scales were more related to  
605 neural response patterns of the OFC, potentially indicating that the construct of kinesiophobia is  
606 more related to higher order brain structures associated with anxiety while the FABQ scales are  
607 more related to subcortical defensive responses to fear. The PASS and its subscales failed to  
608 demonstrate a predictive association with fear-related brain response patterns. From a clinical  
609 point of view, it might indicate that the various PRF questionnaires, although often correlating,  
610 indeed measure different fear phenotypes related to pain. Therefore, the results emphasize the

611 need to carefully consider the different PRF questionnaires in research and clinical settings as  
 612 their constructs do not appear interchangeable.

Table 1. Patient characteristics and descriptive statistics of questionnaires. Tampa Scale of Kinesiophobia (TSK, SF = somatic focus subscale, AA = activity avoidance subscale), Pain Anxiety Symptom Scale (PASS, PASSc = cognitive anxiety, PASSe = escape/avoidance, PASSf = fear, PASSp = physiology), Fear Avoidance Beliefs (FABQ, FABQ-PA = physical activity, FABQ-W = work), State-Trait Anxiety Inventory (S-Anxiety, T-Anxiety).

	<i>Minimum</i>	<i>Maximum</i>	<i>Mean</i>	<i>SD</i>
<b><i>cLBP patients (N = 20, 7 females)</i></b>				
<i>Age</i>	21	62	39,35	13,97
<i>TSK-17</i>	26	52	36,90	5,59
<i>TSK-13</i>	16	43	27,60	5,96
<i>TSK-11</i>	13	38	23,20	5,71
<i>TSK-11-SF</i>	5	16	9,70	2,69
<i>TSK-11-AA</i>	5	20	11,90	3,35
<i>PASS</i>	13	68	38,15	16,57
<i>PASS-C</i>	1	15	8,70	4,19
<i>PASS-E</i>	3	21	9,85	4,77
<i>PASS-F</i>	2	20	9,45	5,28
<i>PASS-P</i>	0	15	7,35	4,21
<i>FABQ</i>	3	83	35,45	22,53
<i>FABQ-PA</i>	2	21	12,80	5,59
<i>FABQ-W</i>	0	40	15,50	12,12
<i>S-Anxiety</i>	36	53	43,70	4,78
<i>T-Anxiety</i>	31	59	43,00	6,05
<i>PainDETECT current pain</i>	0	8	3,77	2,49
<i>PainDETECT strongest pain</i>	2	10	6,15	2,16
<i>PainDETECT average pain (previous 4 weeks)</i>	1	7	3,75	1,88
<i>Ratings harmful activities</i>	0	10	5,44	2,38
<i>Ratings harmless activities</i>	0	5	1,28	1,32

613

614 Table 2. Spearman's rank correlations between the different pain-related fear questionnaires. Tampa Scale of Kinesiophobia (TSK, SF = somatic focus subscale, AA = activity  
 615 avoidance subscale), Pain Anxiety Symptom Scale (PASS = total score, PASS-C = cognitive anxiety, PASS-E = escape/avoidance, PASS-F = fear, PASS-P = physiology), Fear  
 616 Avoidance Beliefs (FABQ = total score, FABQ-PA = physical activity, FABQ-W = work), State and Trait Anxiety Inventory (S-Anxiety, T-Anxiety). \*\*p < 0.005 (bold), \*p < 0.05  
 617 (bold).

		TSK-17	TSK-13	TSK-11	TSK-11_SF	TSK-11_AA	PASS	PASS-C	PASS-E	PASS-F	PASS-P	FABQ	FABQ-PA	FABQ-W	S-ANXIETY	T-ANXIETY	Rating harmful	Rating harmless
TSK-17	Corr.coeff.	1.000	<b>.834**</b>	<b>.800**</b>	<b>.609**</b>	<b>.759**</b>	<b>.611**</b>	<b>.503*</b>	<b>.614**</b>	<b>.556*</b>	<b>.647**</b>	.337	<b>.494*</b>	.280	<b>.449*</b>	.299	.133	.289
	Sig.		<b>.000</b>	<b>.000</b>	<b>.004</b>	<b>.000</b>	<b>.004</b>	<b>.024</b>	<b>.004</b>	<b>.011</b>	<b>.002</b>	.146	<b>.027</b>	.231	<b>.047</b>	.200	.577	.216
TSK-13	Corr.coeff.	<b>.834**</b>	1.000	<b>.960**</b>	<b>.754**</b>	<b>.789**</b>	<b>.686**</b>	<b>.559*</b>	<b>.777**</b>	<b>.666**</b>	<b>.558*</b>	.344	<b>.442*</b>	.339	<b>.451*</b>	.139	.240	.168
	Sig.	<b>.000</b>		<b>.000</b>	<b>.000</b>	<b>.000</b>	<b>.001</b>	<b>.010</b>	<b>.000</b>	<b>.001</b>	<b>.011</b>	.138	<b>.050</b>	.144	<b>.046</b>	.558	.307	.479
TSK-11	Corr.coeff.	<b>.800**</b>	<b>.960**</b>	1.000	<b>.793**</b>	<b>.779**</b>	<b>.685**</b>	<b>.559*</b>	<b>.766**</b>	<b>.643**</b>	<b>.565**</b>	.360	.404	.378	<b>.470*</b>	.071	.276	.091
	Sig.	<b>.000</b>	<b>.000</b>		<b>.000</b>	<b>.000</b>	<b>.001</b>	<b>.010</b>	<b>.000</b>	<b>.002</b>	<b>.009</b>	.120	.077	.101	<b>.037</b>	.766	.238	.703
TSK-11_SF	Corr.coeff.	<b>.609**</b>	<b>.754**</b>	<b>.793**</b>	1.000	.350	<b>.519*</b>	<b>.462*</b>	<b>.529*</b>	<b>.502*</b>	<b>.502*</b>	.351	.315	.411	<b>.629**</b>	.034	.044	.178
	Sig.	<b>.004</b>	<b>.000</b>	<b>.000</b>		.131	<b>.019</b>	<b>.040</b>	<b>.016</b>	<b>.024</b>	<b>.024</b>	.130	.176	.071	<b>.003</b>	.886	.854	.452
TSK-11_AA	Corr.coeff.	<b>.759**</b>	<b>.789**</b>	<b>.779**</b>	.350	1.000	<b>.477**</b>	.268	<b>.564**</b>	<b>.486*</b>	.421	.336	.375	.280	.284	.035	.270	.135
	Sig.	<b>.000</b>	<b>.000</b>	<b>.000</b>	.131		<b>.034</b>	.254	<b>.010</b>	<b>.030</b>	.065	.147	.103	.231	.224	.883	.250	.570
PASS	Corr.coeff.	<b>.611**</b>	<b>.686**</b>	<b>.685**</b>	<b>.519*</b>	<b>.477*</b>	1.000	<b>.895**</b>	<b>.899**</b>	<b>.886**</b>	<b>.801**</b>	.415	<b>.535*</b>	.400	.320	.156	.317	-.118
	Sig.	<b>.004</b>	<b>.001</b>	<b>.001</b>	<b>.019</b>	<b>.034</b>		<b>.000</b>	<b>.000</b>	<b>.000</b>	<b>.000</b>	.069	<b>.015</b>	.081	.168	.510	.173	.620
PASS-C	Corr.coeff.	<b>.503*</b>	<b>.559*</b>	<b>.559*</b>	<b>.462*</b>	.268	<b>.895**</b>	1.000	<b>.737**</b>	<b>.690**</b>	<b>.707**</b>	.329	.424	.344	.227	.118	.214	-.254
	Sig.	<b>.024</b>	<b>.010</b>	<b>.010</b>	<b>.040</b>	.254	<b>.000</b>		<b>.000</b>	<b>.001</b>	<b>.000</b>	.157	.063	.137	.336	.621	.366	.280
PASS-E	Corr.coeff.	<b>.614**</b>	<b>.777**</b>	<b>.766**</b>	<b>.529*</b>	<b>.564**</b>	<b>.899**</b>	<b>.737**</b>	1.000	<b>.918**</b>	<b>.544*</b>	<b>.472*</b>	<b>.592**</b>	.419	.387	.161	.330	-.062
	Sig.	<b>.004</b>	<b>.000</b>	<b>.000</b>	<b>.016</b>	<b>.010</b>	<b>.000</b>	<b>.000</b>		<b>.000</b>	<b>.013</b>	<b>.036</b>	<b>.006</b>	.066	.092	.499	.156	.795
PASS-F	Corr.coeff.	<b>.556*</b>	<b>.666**</b>	<b>.643**</b>	<b>.502*</b>	<b>.486*</b>	<b>.886**</b>	<b>.690**</b>	<b>.918**</b>	1.000	<b>.541*</b>	<b>.577**</b>	<b>.736**</b>	<b>.486*</b>	.291	.188	<b>.445*</b>	.085
	Sig.	<b>.011</b>	<b>.001</b>	<b>.002</b>	<b>.024</b>	<b>.030</b>	<b>.000</b>	<b>.001</b>	<b>.000</b>		<b>.014</b>	<b>.008</b>	<b>.000</b>	<b>.030</b>	.213	.428	<b>.049</b>	.720
PASS-P	Corr.coeff.	<b>.647**</b>	<b>.558*</b>	<b>.565**</b>	<b>.502*</b>	.421	<b>.801**</b>	<b>.707**</b>	<b>.544*</b>	<b>.541*</b>	1.000	.261	.304	.328	.289	.112	.118	-.023
	Sig.	<b>.002</b>	<b>.011</b>	<b>.009</b>	<b>.024</b>	.065	<b>.000</b>	<b>.000</b>	<b>.013</b>	<b>.014</b>		.267	.193	.157	.216	.639	.619	.925
FABQ	Corr.coeff.	.337	.344	.360	.351	.336	.415	.329	<b>.472*</b>	<b>.577**</b>	.261	1.000	<b>.781**</b>	<b>.951**</b>	.314	-.032	.195	.009
	Sig.	.146	.138	.120	.130	.147	.069	.157	<b>.036</b>	<b>.008</b>	.267		<b>.000</b>	<b>.000</b>	.178	.894	.410	.970
FABQ-PA	Corr.coeff.	<b>.494*</b>	<b>.442*</b>	.404	.315	.375	<b>.535*</b>	.424	<b>.592**</b>	<b>.736**</b>	.304	<b>.781**</b>	1.000	<b>.638**</b>	.140	.009	.377	.178
	Sig.	<b>.027</b>	<b>.050</b>	.077	.176	.103	<b>.015</b>	.063	<b>.006</b>	<b>.000</b>	.193	<b>.000</b>	<b>.002</b>	<b>.557</b>	.969	.101	.452	
FABQ-W	Corr.coeff.	.280	.339	.378	.411	.280	.400	.344	.419	<b>.486*</b>	.328	<b>.951**</b>	<b>.638**</b>	1.000	.291	-.069	.185	-.040
	Sig.	.231	.144	.101	.071	.231	.081	.137	.066	<b>.030</b>	.157	<b>.000</b>	<b>.002</b>		.213	.772	.435	.867
S-ANXIETY	Corr.coeff.	<b>.449*</b>	<b>.451*</b>	<b>.470*</b>	<b>.629**</b>	.284	.320	.227	.387	.291	.289	.314	.140	.291	1.000	.128	-.198	.090
	Sig.	<b>.047</b>	<b>.046</b>	<b>.037</b>	<b>.003</b>	.224	.168	.336	.092	.213	.216	.178	.557	.213		.592	.402	.707
T-ANXIETY	Corr.coeff.	.299	.139	.071	.034	.035	.156	.118	.161	.188	.112	-.032	.009	-.069	.128	1.000	.185	.378
	Sig.	.200	.558	.766	.886	.883	.510	.621	.499	.428	.639	.894	.969	.772	.592		.435	.100
Rating harmful	Corr.coeff.	.133	.240	.276	.044	.270	.317	.214	.330	<b>.445*</b>	.118	.195	.377	.185	-.198	.185	1.000	.289
	Sig.	.577	.307	.238	.854	.250	.173	.366	.156	<b>.049</b>	.619	.410	.101	.435	.402	.435		.217
Rating harmless	Corr.coeff.	.289	.168	.091	.178	.135	-.118	-.254	-.062	.085	-.023	.009	.178	-.040	.090	.378	1.000	.289
	Sig.	.216	.479	.703	.452	.570	.620	.280	.795	.720	.925	.970	.452	.867	.707	.100		.217

618

619

620 Table 3A. Model performances of the different MKL models (characterized by the pearson correlation coefficient ( $r$ ) and normalized mean squared error (nMSE).  
 621 Bold:  $p < 0.05$ , \*:  $p < 0.05$ , corrected for multiple comparisons (FDR of 5%).

MKL model	$r$	$p$ -value	nMSE	$p$ -value
<i>FABQ total</i>	<b>0.61</b>	<b>0.012*</b>	<b>4.25</b>	<b>0.014</b>
<i>FABQ-W</i>	<b>0.74</b>	<b>0.004*</b>	<b>1.81</b>	<b>0.003*</b>
<i>FABQ-PA</i>	0.03	0.162	1.68	0.161
<i>TSK-17</i>	0.19	0.098	1.10	0.091
<i>TSK-13</i>	<b>0.37</b>	<b>0.034</b>	<b>1.09</b>	<b>0.033</b>
<i>TSK-11</i>	<b>0.63</b>	<b>0.009*</b>	<b>0.90</b>	<b>0.032</b>
<i>TSK-11-SF</i>	-0.73	0.832	0.86	0.773
<i>TSK-11-AA</i>	-0.63	0.908	0.88	0.879
<i>PASS</i>	0.18	0.119	4.63	0.115
<i>PASS-C</i>	-0.44	0.515	1.64	0.513
<i>PASS-E</i>	-0.32	0.339	1.38	0.331
<i>PASS-F</i>	-0.15	0.259	1.70	0.251
<i>PASS-P</i>	-0.51	0.518	1.36	0.512
<i>T-Anxiety</i>	<b>0.48</b>	<b>0.011*</b>	<b>1.01</b>	<b>0.015</b>
<i>S-Anxiety</i>	-0.46	0.481	1.51	0.475
<i>Ratings harmful activities</i>	-0.01	0.247	0.64	0.242
<i>Ratings harmless activities</i>	-0.72	0.481	0.38	0.441

622

623 Table 3B. Model performances of the between-model cross-validation (characterized by the pearson correlation coefficient ( $r$ ) and normalized  
 624 mean squared error (nMSE). Bold:  $p < 0.05$ , \*:  $p < 0.05$ , corrected for multiple comparisons (FDR of 5%).

<b>Feature set</b>	FABQ total labels	FABQ-W labels	TSK-11 labels	TSK-13 labels	T-Anxiety labels
<i>FABQ total</i>	-	<b><math>r = 0.72, p = 0.001^*</math>, nMSE = 3.29, p = 0.001*</b>	$r = -0.42, p = 0.68$ nMSE = 1.30, p = 0.69	$r = -0.65, p = 0.91$ nMSE = 1.48, p = 0.86	$r = -0.32, p = 0.42$ nMSE = 1.56, p = 0.66
<i>FABQ-W</i>	<b><math>r = 0.8, p = 0.001^*</math>, nMSE = 1.63, p = 0.001*</b>	-	$r = -0.40, p = 0.59$ , nMSE = 1.26, p = 0.47	$r = -0.06, p = 0.25$ nMSE = 4.08, p = 0.24	$r = -0.32, p = 0.42$ nMSE = 1.56, p = 0.66
<i>TSK-11</i>	$r = 0.17, p = 0.12$ , nMSE = 6.27, p = 0.13	$r = -0.06, p = 0.26$ , nMSE = 4.08, p = 0.26	-	<b><math>r = 0.83, p = 0.001^*</math></b> nMSE = 0.57, p = 0.002*	$r = -0.39, p = 0.57$ nMSE = 1.74, p = 0.96
<i>TSK-13</i>	$r = 0.04, p = 0.18$ , nMSE = 7.16, p = 0.32	$r = -0.06, p = 0.31$ , nMSE = 4.08, p = 0.27	<b><math>r = 0.83, p = 0.001^*</math></b> nMSE = 0.57, p = 0.001*	-	$r = -0.37, p = 0.47$ nMSE = 1.78, p = 0.98
<i>T-Anxiety</i>	$r = 0.23, p = 0.11$ , nMSE = 6.01, p = 0.11	$r = 0.2, p = 0.21$ , nMSE = 3.43, p = 0.25	$r = -0.25, p = 0.41$ , nMSE = 1.35, p = 0.81	$r = -0.24, p = 0.41$ , nMSE = 1.45, p = 0.83	-

625 Table 4. Condition and region weights showing the contribution of the two different conditions and fear-related brain regions to  
 626 the final decision function of each MKL model (questionnaires A-E with model performance  $p < 0.05$ , FDR- and uncorrected,  
 627 see Figure 1) in hierarchical order. The brain regions (left and right hemisphere) were parcellated according to the AAL atlas:  
 628 Medial orbitofrontal regions (mOFC: Rectus, Frontal\_Sup\_Orb, Frontal\_Med\_Orb), lateral orbitofrontal regions (lOFC:  
 629 Frontal\_Mid\_Orb, Frontal\_Inf\_Orb), medial prefrontal cortex (mPFC: Frontal\_Sup\_Medial), anterior cingulate cortex  
 630 (Cingulum\_Ant), Thalamus, Amygdala, Hippocampus and Insula. ER = expected ranking. \*brain regions included in the feature  
 631 set for between model cross-validation (see Table 3B for results)

A. FABQ total								
Rank	Harmful activities Brain region <i>AAL label</i>	Condition weight 88%			Harmless activities Brain region <i>AAL label</i>	Condition weight 12%		
		Region size (vox)	Region weight (%)	ER		Region size (vox)	Region weight (%)	ER
1	Thalamus_L*	519	27.25	1.8	Amygdala_R*	96	11.06	0.95
2	Amygdala_R*	96	24.69	1.6	Hippocampus_R	424	0.61	14.70
3	Hippocampus_L*	400	17.29	2.6	Amygdala_L	97	0.43	18.10

632

4	Frontal_Med_Orb_R	413	9.56	4.0	Frontal_Inf_Orb_L	714	0.19	5.15
5	Frontal_Inf_Orb_R	744	6.39	6.1	Frontal_Sup_Orb_L	451	0.00	2.35
6	Frontal_Med_Orb_L	324	2.17	7.5	Frontal_Sup_Orb_R	469	0.00	3.30
7	Hippocampus_R	424	0.31	8.2	Frontal_Mid_Orb_L	408	0.00	4.25
8	Frontal_Sup_Orb_L	451	0.00	6.1	Frontal_Mid_Orb_R	444	0.00	5.20
9	Frontal_Sup_Orb_R	469	0.00	7.0	Frontal_Inf_Orb_R	744	0.00	6.90
10	Frontal_Mid_Orb_L	408	0.00	8.0	Frontal_Sup_Medial_L	1417	0.00	7.85
11	Frontal_Mid_Orb_R	444	0.00	8.9	Frontal_Sup_Medial_R	1006	0.00	8.80
12	Frontal_Inf_Orb_L	714	0.00	9.9	Frontal_Med_Orb_L	324	0.00	9.75
13	Frontal_Sup_Medial_L	1417	0.00	11.1	Frontal_Med_Orb_R	413	0.00	10.70
14	Frontal_Sup_Medial_R	1006	0.00	12.1	Rectus_L	381	0.00	11.65
15	Rectus_L	381	0.00	13.3	Rectus_R	352	0.00	12.60
16	Rectus_R	352	0.00	14.3	Insula_L	887	0.00	13.55
17	Insula_L	887	0.00	15.2	Insula_R	821	0.00	14.50
18	Insula_R	821	0.00	16.2	Cingulum_Ant_L	599	0.00	15.45
19	Cingulum_Ant_L	599	0.00	17.1	Cingulum_Ant_R	639	0.00	16.40
20	Cingulum_Ant_R	639	0.00	18.1	Hippocampus_L	400	0.00	17.35
21	Amygdala_L	97	0.00	19.9	Thalamus_L	519	0.00	19.95
22	Thalamus_R	478	0.00	20.9	Thalamus_R	478	0.00	20.90

633

634

635

636

637

638

639

B. FABQ-W								
Rank	Harmful activities Brain region <i>AAL label</i>	Condition weight 87%			Harmless activities Brain region <i>AAL label</i>	Condition weight 13%		
		Region size (vox)	Region weight (%)	ER		Region size (vox)	Region weight (%)	ER
1	Amygdala_R*	96	40.20	1.40	Amygdala_R*	96	11.82	1.05
2	Thalamus_L*	519	39.42	1.45	Hippocampus_R	424	0.64	16.21
3	Frontal_Med_Orb_L	324	4.17	4.90	Frontal_Med_Orb_L	324	0.22	7.57
4	Frontal_Med_Orb_R	413	2.42	7.25	Cingulum_Ant_R	639	0.16	14.52
5	Hippocampus_L	400	0.52	16.55	Frontal_Sup_Orb_L	451	0.00	2.36
6	Cingulum_Ant_R	639	0.24	16.50	Frontal_Sup_Orb_R	469	0.00	3.31
7	Thalamus_R	478	0.13	20.00	Frontal_Mid_Orb_L	408	0.00	4.26
8	Frontal_Sup_Orb_L	451	0.00	4.30	Frontal_Mid_Orb_R	444	0.00	5.21
9	Frontal_Sup_Orb_R	469	0.00	5.25	Frontal_Inf_Orb_L	714	0.00	6.15

640  
641  
642  
643  
644  
645  
646  
647  
648  
649  
650  
651

10	Frontal_Mid_Orb_L	408	0.00	6.20	Frontal_Inf_Orb_R	744	0.00	7.10
11	Frontal_Mid_Orb_R	444	0.00	7.15	Frontal_Sup_Medial_L	1417	0.00	8.05
12	Frontal_Inf_Orb_L	714	0.00	8.10	Frontal_Sup_Medial_R	1006	0.00	9.00
13	Frontal_Inf_Orb_R	744	0.00	9.05	Frontal_Med_Orb_R	413	0.00	10.63
14	Frontal_Sup_Medial_L	1417	0.00	10.00	Rectus_L	381	0.00	11.57
15	Frontal_Sup_Medial_R	1006	0.00	10.95	Rectus_R	352	0.00	12.52
16	Rectus_L	381	0.00	12.55	Insula_L	887	0.00	13.47
17	Rectus_R	352	0.00	13.50	Insula_R	821	0.00	14.42
18	Insula_L	887	0.00	14.45	Cingulum_Ant_L	599	0.00	15.36
19	Insula_R	821	0.00	15.40	Hippocampus_L	400	0.00	17.15
20	Cingulum_Ant_L	599	0.00	16.35	Amygdala_L	97	0.00	18.94
21	Hippocampus_R	424	0.00	19.05	Thalamus_L	519	0.00	19.89
22	Amygdala_L	97	0.00	20.00	Thalamus_R	478	0.00	20.84

C. TSK-13									
Rank	Harmful activities Brain region AAL label	Condition weight 60%			ER	Harmless activities Brain region AAL label	Condition weight 40%		
		Region size (vox)	Region weight (%)	ER			Region size (vox)	Region weight (%)	ER
1	Frontal_Inf_Orb_R*	744	52.70	1.55	Rectus_L*	381	19.51	2.00	
2	Rectus_L	381	2.37	6.00	Hippocampus_R*	424	14.03	1.80	
3	Insula_L	887	1.33	8.90	Amygdala_L	97	2.34	16.40	
4	Hippocampus_L	400	0.67	14.05	Cingulum_Ant_L	599	1.09	13.95	
5	Insula_R	821	0.62	11.55	Rectus_R	352	0.59	11.65	
6	Amygdala_R	96	0.33	17.10	Frontal_Sup_Orb_R	469	0.44	4.50	
7	Frontal_Mid_Orb_R	444	0.12	5.60	Hippocampus_L	400	0.41	15.85	
8	Frontal_Med_Orb_R	413	0.12	10.35	Thalamus_R	478	0.14	19.55	
9	Hippocampus_R	424	0.12	16.50	Frontal_Med_Orb_R	413	0.12	11.25	

652  
653  
654  
655  
656  
657  
658  
659  
660  
661  
662  
663

10	Frontal_Med_Orb_L	324	0.12	9.60	Amygdala_R	96	0.12	18.40
11	Frontal_Inf_Orb_L	714	0.12	6.95	Frontal_Inf_Orb_L	714	0.12	6.95
12	Thalamus_R	478	0.11	20.25	Frontal_Inf_Orb_R	744	0.12	7.90
13	Frontal_Sup_Medial_L	1417	0.11	8.05	Frontal_Sup_Orb_L	451	0.12	3.50
14	Rectus_R	352	0.11	12.15	Frontal_Sup_Medial_L	1417	0.12	8.90
15	Amygdala_L	97	0.11	17.90	Cingulum_Ant_R	639	0.12	16.10
16	Frontal_Sup_Medial_R	1006	0.11	9.20	Frontal_Mid_Orb_R	444	0.12	6.30
17	Frontal_Mid_Orb_L	408	0.11	5.650	Thalamus_L	519	0.11	19.75
18	Thalamus_L	519	0.11	19.80	Frontal_Med_Orb_L	324	0.11	11.00
19	Cingulum_Ant_R	639	0.11	15.50	Insula_R	821	0.11	14.65
20	Frontal_Sup_Orb_R	469	0.11	4.90	Insula_L	887	0.11	13.80
21	Cingulum_Ant_L	599	0.11	14.70	Frontal_Sup_Medial_R	1006	0.11	10.30
22	Frontal_Sup_Orb_L	451	0.00	4.10	Frontal_Mid_Orb_L	408	0.11	5.85

D. TSK-11									
Rank	Harmful activities Brain region AAL label	Condition weight 66%			ER	Harmless activities Brain region AAL label	Condition weight 34%		
		Region size (vox)	Region weight (%)				Region size (vox)	Region weight (%)	
1	Frontal_Inf_Orb_R*	744	60.49	1.05	Rectus_L*	381	21.29	1.60	
2	Insula_L	887	0.90	11.15	Hippocampus_R*	424	10.41	1.90	
3	Amygdala_R	96	0.65	17.20	Thalamus_L	97	0.41	17.60	
4	Hippocampus_L	400	0.61	14.95	Amygdala_L	599	0.12	17.25	
5	Amygdala_L	97	0.56	17.00	Cingulum_Ant_L	352	0.12	14.65	
6	Insula_R	821	0.46	12.55	Thalamus_R	469	0.11	20.00	
7	Frontal_Med_Orb_R	413	0.34	9.35	Frontal_Mid_Orb_R	400	0.11	5.75	
8	Frontal_Mid_Orb_R	444	0.12	4.90	Cingulum_Ant_R	478	0.11	15.70	
9	Frontal_Med_Orb_L	324	0.12	8.65	Frontal_Sup_Medial_L	413	0.11	8.55	

664  
665  
666  
667  
668  
669  
670  
671  
672  
673  
674  
675

10	Hippocampus_R	424	0.11	16.55	Amygdala_R	96	0.11	18.50
11	Rectus_L	381	0.11	10.70	Hippocampus_L	714	0.11	16.75
12	Frontal_Inf_Orb_L	714	0.11	6.30	Frontal_Med_Orb_R	744	0.11	11.45
13	Thalamus_R	478	0.11	20.40	Frontal_Inf_Orb_L	451	0.11	7.00
14	Rectus_R	352	0.11	11.75	Frontal_Sup_Orb_L	1417	0.11	3.45
15	Frontal_Sup_Medial_R	1006	0.11	8.30	Frontal_Inf_Orb_R	639	0.11	8.05
16	Cingulum_Ant_R	639	0.11	15.35	Frontal_Sup_Medial_R	444	0.11	9.90
17	Frontal_Sup_Medial_L	1417	0.11	7.50	Rectus_R	519	0.11	12.65
18	Cingulum_Ant_L	599	0.11	14.55	Insula_R	324	0.11	14.50
19	Frontal_Mid_Orb_L	408	0.11	4.90	Frontal_Sup_Orb_R	821	0.11	4.65
20	Thalamus_L	519	0.11	19.90	Frontal_Mid_Orb_L	887	0.10	5.60
21	Frontal_Sup_Orb_R	469	0.10	4.10	Insula_L	1006	0.10	13.75
22	Frontal_Sup_Orb_L	451	0.00	3.25	Frontal_Med_Orb_L	408	0.10	11.10

E. T-Anxiety									
Rank	Harmful activities Brain region AAL label	Condition weight 52%			ER	Harmless activities Brain region AAL label	Condition weight 48%		
		Region size (vox)	Region weight (%)				Region size (vox)	Region weight (%)	ER
1	Frontal_Sup_Medial_L*	1417	20.20	1.95	Frontal_Med_Orb_L*	324	20.86	1.05	
2	Frontal_Med_Orb_L*	324	13.82	1.90	Thalamus_L*	519	13.29	3.75	
3	Rectus_L	381	9.97	3.25	Frontal_Sup_Orb_R	469	9.87	2.85	
4	Frontal_Mid_Orb_R	444	3.48	7.30	Amygdala_L	97	2.06	10.15	
5	Insula_R	821	2.85	6.90	Amygdala_R	96	0.44	18.95	
6	Rectus_R	352	0.98	10.40	Frontal_Sup_Medial_L	1417	0.40	9.15	
7	Cingulum_Ant_R	639	0.87	14.50	Frontal_Mid_Orb_R	444	0.23	6.30	
8	Amygdala_L	97	0.25	17.35	Cingulum_Ant_R	639	0.06	15.95	
9	Frontal_Inf_Orb_R	744	0.22	9.00	Hippocampus_L	400	0.00	16.95	

10	Amygdala_R	96	0.07	19.00	Frontal_Sup_Orb_L	451	0.00	4.35
11	Frontal_Sup_Orb_L	451	0.00	4.70	Frontal_Mid_Orb_L	408	0.00	5.35
12	Frontal_Sup_Orb_R	469	0.00	5.65	Frontal_Inf_Orb_L	714	0.00	7.25
13	Frontal_Mid_Orb_L	408	0.00	6.60	Frontal_Inf_Orb_R	744	0.00	8.20
14	Frontal_Inf_Orb_L	714	0.00	8.45	Frontal_Sup_Medial_R	1006	0.00	10.10
15	Frontal_Sup_Medial_R	1006	0.00	10.40	Frontal_Med_Orb_R	413	0.00	11.05
16	Frontal_Med_Orb_R	413	0.00	11.35	Rectus_L	381	0.00	12.00
17	Insula_L	887	0.00	13.10	Rectus_R	352	0.00	12.95
18	Cingulum_Ant_L	599	0.00	14.35	Insula_L	887	0.00	13.90
19	Hippocampus_L	400	0.00	16.20	Insula_R	821	0.00	14.85
20	Hippocampus_R	424	0.00	17.15	Cingulum_Ant_L	599	0.00	15.80
21	Thalamus_L	519	0.00	19.95	Hippocampus_R	424	0.00	18.55
22	Thalamus_R	478	0.00	20.90	Thalamus_R	478	0.00	20.90

676

677

678

679

680

681

682

683

684

685 **Figure legends**

686 Figure 1. The model performance ( $r$ , MSE) characterizes the strength of relationship between  
687 true and predicted labels. Condition and region weights show the predictive contribution of the  
688 two different conditions (harmful, harmless) and fear-related brain regions (parcellated according  
689 to the AAL atlas, L = left, R = right) to the final decision function of each MKL model

690 (questionnaires A-E with model performance  $p < 0.05$ , FDR- and uncorrected). Brain regions  
691 (feature set): Thalamus (1), Hippocampus (2), Amygdala (3), Insula (4), mOFC: Rectus (5),  
692 Frontal\_Sup\_Orb (6), Frontal\_Med\_Orb (7), lateral OFC: Frontal\_Mid\_Orb (8), Frontal\_Inf\_Orb  
693 (9), mPFC: Frontal\_Sup\_Medial (10), anterior cingulate cortex (Cingulum\_Ant (11).  
694 indicates not visible contralateral homologue.

695

696

697

698

699

700

701

702

703 References

704 Altman DG, Royston P (2006) The cost of dichotomising continuous variables. *BMJ (Clinical*  
705 *research ed.)* 332:1080.

706 Anderson AK, Phelps EA (2002) Is the human amygdala critical for the subjective experience of  
707 emotion? Evidence of intact dispositional affect in patients with amygdala lesions. *Journal of*  
708 *cognitive neuroscience* 14:709–720.

- 709 Aue T, Hoeppli M-E, Piguet C, Hofstetter C, Rieger SW, Vuilleumier P (2015) Brain systems  
710 underlying encounter expectancy bias in spider phobia. *Cognitive, affective & behavioral*  
711 *neuroscience* 15:335–348.
- 712 Avants BB, Epstein CL, Grossman M, Gee JC (2008) Symmetric diffeomorphic image  
713 registration with cross-correlation. Evaluating automated labeling of elderly and  
714 neurodegenerative brain. *Medical image analysis* 12:26–41.
- 715 Barke A, Preis MA, Schmidt-Samoa C, Baudewig J, Kröner-Herwig B, Dechent P (2016) Neural  
716 Correlates Differ in High and Low Fear-Avoidant Chronic Low Back Pain Patients When  
717 Imagining Back-Straining Movements. *The journal of pain : official journal of the American*  
718 *Pain Society* 17:930–943.
- 719 Behzadi Y, Restom K, Liau J, Liu TT (2007) A component based noise correction method  
720 (CompCor) for BOLD and perfusion based fMRI. *NeuroImage* 37:90–101.
- 721 Berggren N, Blonievsky T, Derakshan N (2015) Enhanced visual detection in trait anxiety.  
722 *Emotion (Washington, D.C.)* 15:477–483.
- 723 Braem S, Houwer J de, Demanet J, Yuen KSL, Kalisch R, Brass M (2017) Pattern Analyses  
724 Reveal Separate Experience-Based Fear Memories in the Human Right Amygdala. *The*  
725 *Journal of neuroscience : the official journal of the Society for Neuroscience* 37:8116–8130.
- 726 Caneiro JP, O'Sullivan P, Smith A, Moseley GL, Lipp OV (2017) Implicit evaluations and  
727 physiological threat responses in people with persistent low back pain and fear of bending.  
728 *Scandinavian journal of pain.*
- 729 Choi BCK, Pak AWP (2005) A catalog of biases in questionnaires. *Preventing chronic disease*  
730 2:A13.

- 731 Cooper AJ, Perkins AM, Corr PJ (2007) A confirmatory factor analytic study of anxiety, fear and  
732 Behavioural Inhibition System measures. *Journal of Individual Differences* 28:179-87.
- 733 Cox RW (1996) AFNI. Software for analysis and visualization of functional magnetic resonance  
734 neuroimages. *Computers and biomedical research, an international journal* 29:162–173.
- 735 Crombez G, Vlaeyen JW, Heuts PH, Lysens R (1999) Pain-related fear is more disabling than  
736 pain itself: evidence on the role of pain-related fear in chronic back pain disability. *Pain*  
737 80:329–339.
- 738 Darwin C (1873) *The expression of the emotions in man and animals*. New York: D. Appleton  
739 and company.
- 740 Deyo RA, Weinstein JN (2001) Low back pain. *The New England journal of medicine* 344:363–  
741 370.
- 742 Dilger S, Straube T, Mentzel H-J, Fitzek C, Reichenbach JR, Hecht H, Krieschel S, Gutberlet I,  
743 Miltner WHR (2003) Brain activation to phobia-related pictures in spider phobic humans. An  
744 event-related functional magnetic resonance imaging study. *Neuroscience letters* 348:29–32.
- 745 Dougherty PE, Karuza J, Savino D, Katz P (2014) Evaluation of a modified clinical prediction  
746 rule for use with spinal manipulative therapy in patients with chronic low back pain. A  
747 randomized clinical trial. *Chiropractic & manual therapies* 22:41.
- 748 Esteve R, Bendayan R, López-Martínez AE, Ramírez-Maestre C (2017) Resilience and  
749 Vulnerability Factors When Pain is Acute as Predictors of Disability: Findings From a Two-  
750 Year Longitudinal Study. *Pain medicine (Malden, Mass.)* 18:2116–2125.
- 751 Fanselow MS, Pennington ZT (2017) The Danger of LeDoux and Pine's Two-System  
752 Framework for Fear. *The American journal of psychiatry* 174:1120–1121.

- 753 Feinstein JS, Buzza C, Hurlmann R, Follmer RL, Dahdaleh NS, Coryell WH, Welsh MJ, Tranel  
754 D, Wemmie JA (2013) Fear and panic in humans with bilateral amygdala damage. *Nature*  
755 *neuroscience* 16:270–272.
- 756 Fernandes O, Portugal LCL, Alves RdCS, Arruda-Sanchez T, Rao A, Volchan E, Pereira M,  
757 Oliveira L, Mourao-Miranda J (2017) Decoding negative affect personality trait from patterns  
758 of brain activation to threat stimuli. *NeuroImage* 145:337–345.
- 759 Flynn T, Fritz J, Whitman J, Wainner R, Magel J, Rendeiro D, Butler B, Garber M, Allison S  
760 (2002) A clinical prediction rule for classifying patients with low back pain who demonstrate  
761 short-term improvement with spinal manipulation. *Spine* 27:2835–2843.
- 762 Formisano E, Martino F de, Valente G (2008) Multivariate analysis of fMRI time series.  
763 Classification and regression of brain responses using machine learning. *Magnetic resonance*  
764 *imaging* 26:921–934.
- 765 Freynhagen R, Baron R, Gockel U, Tolle TR (2006) painDETECT: a new screening  
766 questionnaire to identify neuropathic components in patients with back pain. *Current medical*  
767 *research and opinion* 22:1911–1920.
- 768 George SZ, Bialosky JE, Donald DA (2005) The centralization phenomenon and fear-avoidance  
769 beliefs as prognostic factors for acute low back pain. A preliminary investigation involving  
770 patients classified for specific exercise. *The Journal of orthopaedic and sports physical*  
771 *therapy* 35:580–588.
- 772 George SZ, Fritz JM, Childs JD (2008) Investigation of elevated fear-avoidance beliefs for  
773 patients with low back pain. A secondary analysis involving patients enrolled in physical  
774 therapy clinical trials. *The Journal of orthopaedic and sports physical therapy* 38:50–58.

- 775 Ghasemi A, Zahediasl S (2012) Normality tests for statistical analysis. A guide for non-  
776 statisticians. *International journal of endocrinology and metabolism* 10:486–489.
- 777 Glombiewski JA, Riecke J, Holzapfel S, Rief W, König S, Lachnit H, Seifart U (2015) Do  
778 patients with chronic pain show autonomic arousal when confronted with feared movements?  
779 An experimental investigation of the fear-avoidance model. *Pain* 156:547–554.
- 780 Gorgolewski K, Burns CD, Madison C, Clark D, Halchenko YO, Waskom ML, Ghosh SS (2011)  
781 Nipype. A flexible, lightweight and extensible neuroimaging data processing framework in  
782 python. *Frontiers in neuroinformatics* 5:13.
- 783 Goubert L, Crombez G, van Damme S, Vlaeyen JWS, Bijttebier P, Roelofs J (2004)  
784 Confirmatory factor analysis of the Tampa Scale for Kinesiophobia: invariant two-factor  
785 model across low back pain patients and fibromyalgia patients. *The Clinical journal of pain*  
786 20:103–110.
- 787 Gray JA, MacNaughton N (2000) *The neuropsychology of anxiety. An enquiry into the functions*  
788 *of the septo-hippocampal system.* Oxford: Oxford Univ. Press.
- 789 Greve DN, Fischl B (2009) Accurate and robust brain image alignment using boundary-based  
790 registration. *NeuroImage* 48:63–72.
- 791 Hahn A, Stein P, Windischberger C, Weissenbacher A, Spindelegger C, Moser E, Kasper S,  
792 Lanzenberger R (2011) Reduced resting-state functional connectivity between amygdala and  
793 orbitofrontal cortex in social anxiety disorder. *NeuroImage* 56:881–889.
- 794 Haynes J-D (2015) *A Primer on Pattern-Based Approaches to fMRI. Principles, Pitfalls, and*  
795 *Perspectives.* *Neuron* 87:257–270.
- 796 Hebart MN, Baker CI (2017) Deconstructing multivariate decoding for the study of brain  
797 function. *NeuroImage*.

- 798 Ivanescu AE, Li P, George B, Brown AW, Keith SW, Raju D, Allison DB (2016) The  
799 importance of prediction model validation and assessment in obesity and nutrition research.  
800 *International journal of obesity* (2005) 40:887–894.
- 801 Jenkinson M, Bannister P, Brady M, Smith S (2002) Improved optimization for the robust and  
802 accurate linear registration and motion correction of brain images. *NeuroImage* 17:825–841.
- 803 Julian LJ (2011) Measures of anxiety. State-Trait Anxiety Inventory (STAI), Beck Anxiety  
804 Inventory (BAI), and Hospital Anxiety and Depression Scale-Anxiety (HADS-A). *Arthritis  
805 care & research* 63 Suppl 11:S467-72.
- 806 Kori SH, Miller R.P., Todd D.D. (1990) Kinesophobia: a new view of chronic pain behaviour.  
807 *Pain Management*:35–43.
- 808 Kreddig N, Hasenbring MI (2017) Pain anxiety and fear of (re)injury in patients with chronic  
809 back pain: Sex as a moderator. *Scandinavian journal of pain* 16:105–111.
- 810 Kreddig N, Rusu AC, Burkhardt K, Hasenbring MI (2015) The German PASS-20 in patients  
811 with low back pain. New aspects of convergent, divergent, and criterion-related validity.  
812 *International journal of behavioral medicine* 22:197–205.
- 813 Lara-Vásquez A, Espinosa N, Durán E, Stockle M, Fuentealba P (2016) Midline thalamic  
814 neurons are differentially engaged during hippocampus network oscillations. *Scientific  
815 reports* 6:29807.
- 816 LeDoux JE (2000) Emotion circuits in the brain. *Annual review of neuroscience* 23:155–184.
- 817 LeDoux JE, Hofmann SG (2018) The subjective experience of emotion: a fearful view. *Current  
818 Opinion in Behavioral Sciences*:67–72.
- 819 LeDoux JE, Pine DS (2016) Using Neuroscience to Help Understand Fear and Anxiety. A Two-  
820 System Framework. *The American journal of psychiatry* 173:1083–1093.

- 821 Leeuw M, Goossens MEJB, van Breukelen GJP, Boersma K, Vlaeyen JWS (2007a) Measuring  
822 perceived harmfulness of physical activities in patients with chronic low back pain: the  
823 Photograph Series of Daily Activities--short electronic version. *The journal of pain : official*  
824 *journal of the American Pain Society* 8:840–849.
- 825 Leeuw M, Goossens, Mariëlle E J B, Linton SJ, Crombez G, Boersma K, Vlaeyen JWS (2007b)  
826 The fear-avoidance model of musculoskeletal pain: current state of scientific evidence.  
827 *Journal of behavioral medicine* 30:77–94.
- 828 Leeuw M, Peters ML, Wiers RW, Vlaeyen JWS (2007c) Measuring fear of movement/(re)injury  
829 in chronic low back pain using implicit measures. *Cognitive behaviour therapy* 36:52–64.
- 830 Lundberg M, Grimby-Ekman A, Verbunt J, Simmonds MJ (2011) Pain-related fear: a critical  
831 review of the related measures. *Pain research and treatment* 2011:494196.
- 832 Maher C, Underwood M, Buchbinder R (2017) Non-specific low back pain. *Lancet (London,*  
833 *England)* 389:736–747.
- 834 Marshall PWM, Schabrun S, Knox MF (2017) Physical activity and the mediating effect of fear,  
835 depression, anxiety, and catastrophizing on pain related disability in people with chronic low  
836 back pain. *PloS one* 12:e0180788.
- 837 McCracken LM, Dhingra L (2002) A short version of the Pain Anxiety Symptoms Scale (PASS-  
838 20). Preliminary development and validity. *Pain research & management* 7:45–50.
- 839 McCracken LM, Gross RT, Aikens J, Carnrike CL (1996) The assessment of anxiety and fear in  
840 persons with chronic pain. A comparison of instruments. *Behaviour research and therapy*  
841 34:927–933.
- 842 McNaughton N, Corr PJ (2004) A two-dimensional neuropsychology of defense. Fear/anxiety  
843 and defensive distance. *Neuroscience and biobehavioral reviews* 28:285–305.

- 844 Meier ML, Matos NMP de, Brügger M, Ettlín DA, Lukic N, Cheetham M, Jáncke L, Lutz K  
845 (2014) Equal pain-Unequal fear response. Enhanced susceptibility of tooth pain to fear  
846 conditioning. *Frontiers in human neuroscience* 8:526.
- 847 Meier ML, Stampfli P, Vrana A, Humphreys BK, Seifritz E, Hotz-Boendermaker S (2016)  
848 Neural Correlates of Fear of Movement in Patients with Chronic Low Back Pain vs. Pain-  
849 Free Individuals. *Frontiers in human neuroscience* 10:386.
- 850 Meier ML, Stämpfli P, Humphreys BK, Vrana A, Seifritz E, Schweinhardt P (2017) The impact  
851 of pain-related fear on neural pathways of pain modulation in chronic low back pain. *PAIN*  
852 Reports.
- 853 Mintken PE, Cleland JA, Whitman JM, George SZ (2010) Psychometric properties of the Fear-  
854 Avoidance Beliefs Questionnaire and Tampa Scale of Kinesiophobia in patients with  
855 shoulder pain. *Archives of physical medicine and rehabilitation* 91:1128–1136.
- 856 Neblett R, Hartzell MM, Mayer TG, Bradford EM, Gatchel RJ (2016) Establishing clinically  
857 meaningful severity levels for the Tampa Scale for Kinesiophobia (TSK-13). *European*  
858 *journal of pain (London, England)* 20:701–710.
- 859 Panksepp J (1998) *Affective neuroscience. The foundations of human and animal emotions.* New  
860 York: Oxford University Press.
- 861 Panksepp J (2011) The basic emotional circuits of mammalian brains. Do animals have affective  
862 lives? *Neuroscience and biobehavioral reviews* 35:1791–1804.
- 863 Penzo MA, Robert V, Tucciarone J, Bundel D de, Wang M, van Aelst L, Darvas M, Parada LF,  
864 Palmiter RD, He M, Huang ZJ, Li B (2015) The paraventricular thalamus controls a central  
865 amygdala fear circuit. *Nature* 519:455–459.

- 866 Perkins AM, Kemp SE, Corr PJ (2007) Fear and anxiety as separable emotions. An investigation  
867 of the revised reinforcement sensitivity theory of personality. *Emotion* (Washington, D.C.)  
868 7:252–261.
- 869 Pfingsten M, Kröner-Herwig B, Leibing E, Kronshage U, Hildebrandt J (2000) Validation of the  
870 German version of the Fear-Avoidance Beliefs Questionnaire (FABQ). *European journal of*  
871 *pain* (London, England) 4:259–266.
- 872 Pruim RHR, Mennes M, van Rooij D, Llera A, Buitelaar JK, Beckmann CF (2015) ICA-  
873 AROMA. A robust ICA-based strategy for removing motion artifacts from fMRI data.  
874 *NeuroImage* 112:267–277.
- 875 Qi S, Hassabis D, Sun J, Guo F, Daw N, Mobbs D (2018) How cognitive and reactive fear  
876 circuits optimize escape decisions in humans. *Proceedings of the National Academy of*  
877 *Sciences of the United States of America*.
- 878 Rakotomamonjy A, Bach F, Canu S, Grandvalet Y (2008) Simplemkl. *Journal of Machine*  
879 *Learning Research*:2491–2521.
- 880 Roelofs J, Goubert L, Peters ML, Vlaeyen JWS, Crombez G (2004a) The Tampa Scale for  
881 Kinesiophobia. Further examination of psychometric properties in patients with chronic low  
882 back pain and fibromyalgia. *European journal of pain* (London, England) 8:495–502.
- 883 Roelofs J, McCracken L, Peters ML, Crombez G, van Breukelen G, Vlaeyen JW (2004b)  
884 Psychometric evaluation of the Pain Anxiety Symptoms Scale (PASS) in chronic pain  
885 patients. *Journal of behavioral medicine* 27:167–183.
- 886 Roelofs J, Sluiter JK, Frings-Dresen MHW, Goossens M, Thibault P, Boersma K, Vlaeyen JWS  
887 (2007) Fear of movement and (re)injury in chronic musculoskeletal pain. Evidence for an

- 888 invariant two-factor model of the Tampa Scale for Kinesiophobia across pain diagnoses and  
889 Dutch, Swedish, and Canadian samples. *Pain* 131:181–190.
- 890 Rusu AC, Kreddig N, Hallner D, Hülsebusch J, Hasenbring MI (2014) Fear of  
891 movement/(Re)injury in low back pain: confirmatory validation of a German version of the  
892 Tampa Scale for Kinesiophobia. *BMC musculoskeletal disorders* 15:280.
- 893 Schrouff J, Monteiro JM, Portugal L, Rosa MJ, Phillips C, Mourão-Miranda J (2018) Embedding  
894 Anatomical or Functional Knowledge in Whole-Brain Multiple Kernel Learning Models.  
895 *Neuroinformatics*.
- 896 Schrouff J, Rosa MJ, Rondina JM, Marquand AF, Chu C, Ashburner J, Phillips C, Richiardi J,  
897 Mourão-Miranda J (2013) PRoNTTo. Pattern recognition for neuroimaging toolbox.  
898 *Neuroinformatics* 11:319–337.
- 899 Shackman AJ, Salomons TV, Slagter HA, Fox AS, Winter JJ, Davidson RJ (2011) The  
900 integration of negative affect, pain and cognitive control in the cingulate cortex. *Nature*  
901 *reviews. Neuroscience* 12:154–167.
- 902 Shattuck DW, Leahy RM (2002) BrainSuite. An automated cortical surface identification tool.  
903 *Medical image analysis* 6:129–142.
- 904 Shrout PE, Stadler G, Lane SP, McClure MJ, Jackson GL, Clavél FD, Iida M, Gleason MEJ, Xu  
905 JH, Bolger N (2017) Initial elevation bias in subjective reports. *Proceedings of the National*  
906 *Academy of Sciences of the United States of America*.
- 907 Spielberger CD, Gorsuch RL (1983) *Manual for the State-Trait Anxiety Inventory (Form Y)*.  
908 ("self-evaluation questionnaire"). Palo Alto, CA: Consulting Psychologists Press, Inc.
- 909 Stevens ML, Steffens D, Ferreira ML, Latimer J, Li Q, Blyth F, Maher CG (2016) Patients' and  
910 Physiotherapists' Views on Triggers for Low Back Pain. *Spine* 41:E218-24.

- 911 Tkachuk GA, Harris CA (2012) Psychometric properties of the Tampa Scale for Kinesiophobia-  
912 11 (TSK-11). *The journal of pain : official journal of the American Pain Society* 13:970–977.
- 913 Tovote P, Fadok JP, Lüthi A (2015) Neuronal circuits for fear and anxiety. *Nature reviews.*  
914 *Neuroscience* 16:317–331.
- 915 Trost Z, France CR, Thomas JS (2009) Examination of the photograph series of daily activities  
916 (PHODA) scale in chronic low back pain patients with high and low kinesiophobia. *Pain*  
917 141:276–282.
- 918 Tzourio-Mazoyer N, Landeau B, Papathanassiou D, Crivello F, Etard O, Delcroix N, Mazoyer B,  
919 Joliot M (2002) Automated anatomical labeling of activations in SPM using a macroscopic  
920 anatomical parcellation of the MNI MRI single-subject brain. *NeuroImage* 15:273–289.
- 921 van der Werf YD, Witter MP, Groenewegen HJ (2002) The intralaminar and midline nuclei of  
922 the thalamus. Anatomical and functional evidence for participation in processes of arousal  
923 and awareness. *Brain research. Brain research reviews* 39:107–140.
- 924 Varoquaux G, Thirion B (2014) How machine learning is shaping cognitive neuroimaging.  
925 *GigaScience* 3:28.
- 926 Vlaeyen JW, Kole-Snijders AM, Boeren RG, van Eek H (1995) Fear of movement/(re)injury in  
927 chronic low back pain and its relation to behavioral performance. *Pain* 62:363–372.
- 928 Vlaeyen JW, Linton SJ (2000) Fear-avoidance and its consequences in chronic musculoskeletal  
929 pain: a state of the art. *Pain* 85:317–332.
- 930 Vlaeyen JWS, Crombez G, Linton SJ (2016) The fear-avoidance model of pain. *Pain* 157:1588–  
931 1589.

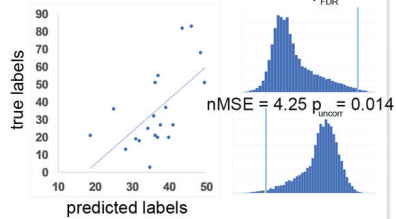
- 932 Waddell G, Newton M, Henderson I, Somerville D, Main CJ (1993) A Fear-Avoidance Beliefs  
933 Questionnaire (FABQ) and the role of fear-avoidance beliefs in chronic low back pain and  
934 disability. *Pain* 52:157–168.
- 935 Wertli MM, Rasmussen-Barr E, Held U, Weiser S, Bachmann LM, Brunner F (2014a) Fear-  
936 avoidance beliefs-a moderator of treatment efficacy in patients with low back pain. A  
937 systematic review. *The spine journal : official journal of the North American Spine Society*  
938 14:2658–2678.
- 939 Wertli MM, Rasmussen-Barr E, Weiser S, Bachmann LM, Brunner F (2014b) The role of fear  
940 avoidance beliefs as a prognostic factor for outcome in patients with nonspecific low back  
941 pain: a systematic review. *The spine journal : official journal of the North American Spine*  
942 *Society* 14:816-36.e4.
- 943 Zhang Y, Brady M, Smith S (2001) Segmentation of brain MR images through a hidden Markov  
944 random field model and the expectation-maximization algorithm. *IEEE transactions on*  
945 *medical imaging* 20:45–57.
- 946 Zheng J, Anderson KL, Leal SL, Shestyuk A, Gulsen G, Mnatsakanyan L, Vadera S, Hsu FPK,  
947 Yassa MA, Knight RT, Lin JJ (2017) Amygdala-hippocampal dynamics during salient  
948 information processing. *Nature communications* 8:14413.
- 949

model performance

null distribution  
16'000 permutations

A. FABQ total

$r = 0.61$   $p_{FDR} = 0.012$



condition weights

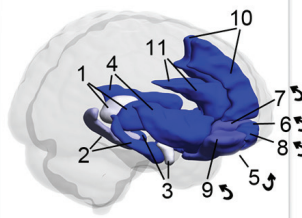


88%



12%

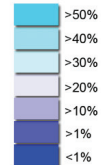
region weights  
harmful



region weights  
harmless

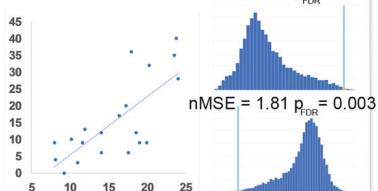


regional neural contribution



B. FABQ work

$r = 0.74$   $p_{FDR} = 0.004$



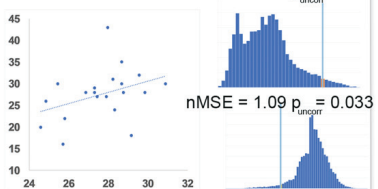
87%



13%

C. TSK-13

$r = 0.37$   $p_{uncorr} = 0.034$



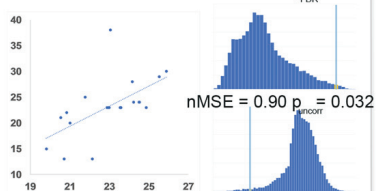
60%



40%

D. TSK-11

$r = 0.60$   $p_{FDR} = 0.009$



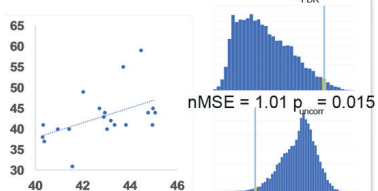
66%



34%

E. T-Anxiety

$r = 0.48$   $p_{FDR} = 0.011$



52%



48%

